Thumbs Up

Development and Validation of a Physical Model of the Trapeziometacarpal Joint

Delphin Jodi Esenkbrink

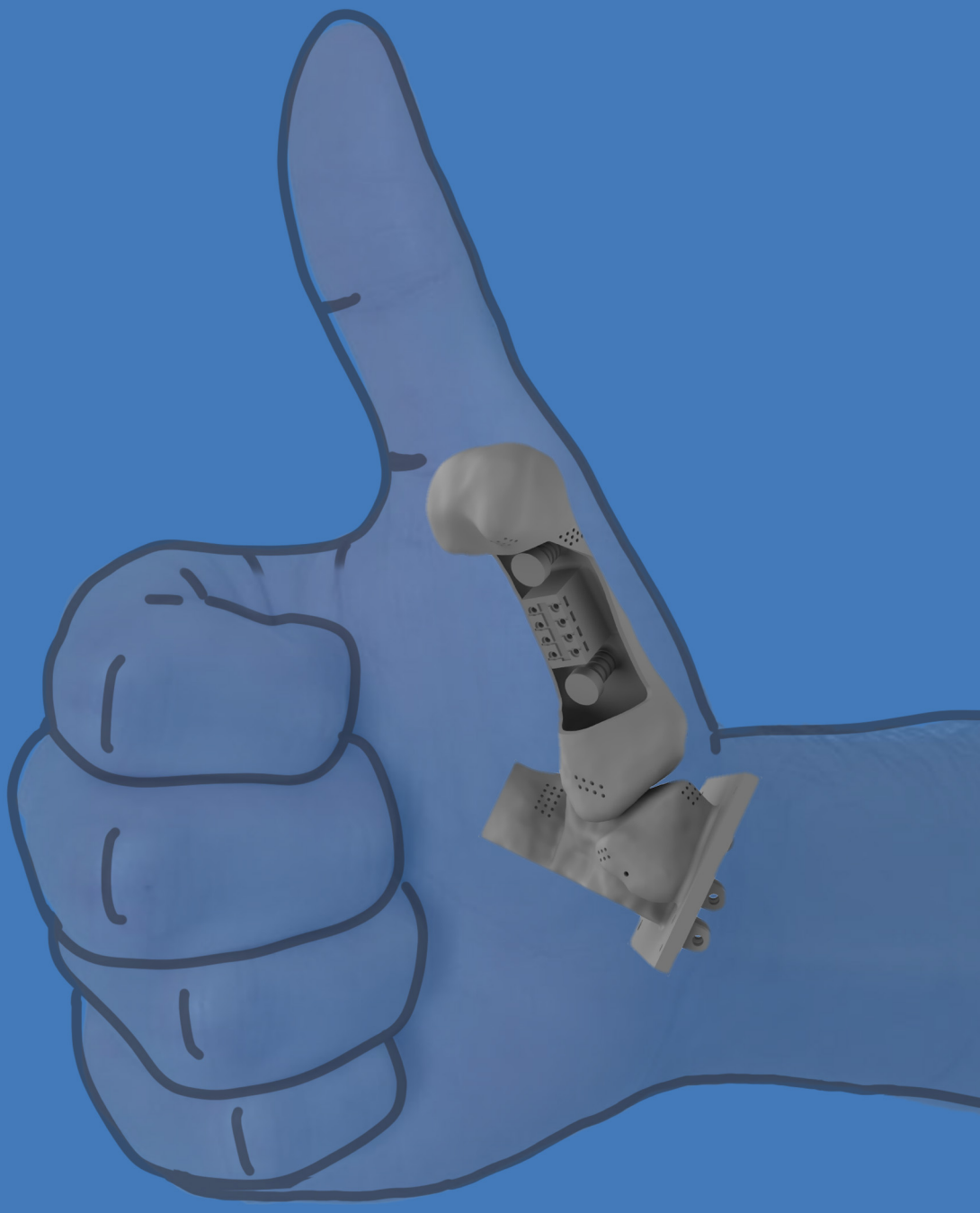

Delft University of Technology

TU Delft

Thumbs Up

Development and Validation of a Physical Model of the Trapeziometacarpal Joint

by

Delphin Jodi Esenkbrink

to obtain the degree of Master of Science
at the Delft University of Technology,
to be defended publicly on Wednesday September 17, 2025

Student number: 4209052

Thesis committee:	Dr. ir. G. Smit,	TU Delft, supervisor
	Dr. G. A. Kraan,	Reinier de Graaf Gasthuis, supervisor
	Dr. ir. A. Seth,	TU Delft, external member

Faculty of Mechanical Engineering

An electronic version of this thesis is available at `http://repository.tudelft.nl/`.

TU Delft

Preface

Ever since I was a child, I have had a profound interest in mechanics. It started out with countless hours building all kinds of things with Lego, K'nex and Meccano. During my many trips to the railway museum—thanks dad for indulging me—I never lost my wonder for the old steam engines. It came as no surprise that I chose to study mechanical engineering at TU Delft. After finishing my bachelor's degree, my fascination with the complexity of nature and its evolution led me to pursue the master track Biomechanical Design.

In my time as a student, I discovered the world of rock climbing. This sport led to several injuries, most of them finger-related. When I got the opportunity to do an internship at the Reinier Haga Orthopedish Centrum concerning hand biomechanics, I grabbed it with both hands. During this time I was allowed to attend surgeries and the outpatient clinic, providing insight into orthopaedics and its role in improving patients daily lives. After the internship my supervisor, Dr. G. A. Kraan, had a thesis project available on thumb stability.

In the course of this thesis project, I experienced many ups and downs. After struggling with my mental wellbeing for so long, I eventually lost faith in myself and the hope of finishing my master's degree. But in these tough times, my supervisors—Dr. Kraan and Dr. Ir. G. Smit—, always kept believing in me and my ability to finish my thesis. I would like to express my sincerest gratitude towards both for not giving up on me and continuously reminding me that I could do it.

Additionally, I would like to thank Ir. J. van Frankenhuyzen for his support during the design and manufacturing of my model. His insights into mechanical systems and 3D printing have proved valuable throughout the thesis project. Finally, my thanks go out to all the people around me—family, friends, roommates, colleagues—that have supported me during my thesis project. Without your support, I would never have made it to the finish.

Delphin Jodi Esenkbrink
Delft, September 2025

Summary

Background The trapeziometacarpal (TMC) joint plays an important role in routine tasks. However, little consensus exists on the composition of its ligaments and their contribution to joint stability. **Aim** This thesis aimed to develop a physical model of the TMC joint to investigate the influence of ligaments on joint stability. **Method** The model was constructed using 3D-printed bones and ligaments represented by Dyneema rope, actuated through tendon routing. Its kinematics were compared to subject-specific in-vivo data from 4D CT. Both active and passive actuation trials were performed. **Results** The model successfully reproduced circumduction motion, but its range of motion deviated from in-vivo results. Active and passive actuation produced comparable outcomes for circumduction, but discrepancies in pure motions revealed an oversimplification of the actuation system. **Conclusion** This thesis presents, to the best of the authors knowledge, the first physical model of the TMC joint. Although simplifications in ligament representation and actuation reduced anatomical accuracy, it lays the foundation for further research and clinical application in thumb biomechanics.

Contents

Preface i

Summary ii

Nomenclature v

1 Introduction 1
- 1.1 Background . . . 1
- 1.2 State of the Art . . . 1
- 1.3 Problem Statement . . . 1
- 1.4 Aim of the Study . . . 2

2 Anatomy 3
- 2.1 Skeletal Structure . . . 3
- 2.2 Ligaments . . . 3
- 2.3 Muscles and Tendons . . . 5

3 Design 6
- 3.1 Design Process . . . 6
- 3.2 Design Criteria . . . 6
- 3.3 Identification of Relevant Ligaments and Tendons . . . 6
- 3.4 Rope Attachment . . . 7
- 3.5 Bone Model . . . 8
  - 3.5.1 Obtaining Bone Geometry . . . 8
  - 3.5.2 MC1 . . . 8
  - 3.5.3 Trapezium . . . 9

4 3D Printing 11
- 4.1 3D Printing Method . . . 11
- 4.2 Material . . . 11
- 4.3 Post-Processing . . . 12

5 Assembly 13
- 5.1 Frame Construction . . . 13
- 5.2 Ligament Routing . . . 13
- 5.3 Tendon Actuation . . . 14

6 Validation 15
- 6.1 Introduction . . . 15
- 6.2 Measurement Protocol . . . 15
- 6.3 Data Analysis . . . 16

7 Results 18
- 7.1 Actively Actuated Motion . . . 18
- 7.2 Passively Actuated Motion . . . 19
- 7.3 Range of Motion . . . 19

8 Discussion 23
- 8.1 Summary of Key Findings . . . 23
- 8.2 Model Performance Compared to In-Vivo Motion . . . 23
  - 8.2.1 Coordinate System Alignment . . . 23
  - 8.2.2 Subject-Specific Anatomy . . . 23
- 8.3 Model Simplifications and Their Implications . . . 23
  - 8.3.1 Ligament Selection . . . 23

8.3.2 Uniform Stiffness . . . 24
8.3.3 Simplified Fibre Architecture and Attachments . . . 24
8.4 Evaluation of the Actuation System . . . 24
8.5 Comparison to Existing Models . . . 25
8.6 Limitations . . . 25
8.6.1 General Limitations . . . 25
8.6.2 Design and Validation Limits . . . 25
8.7 Recommendations . . . 25
8.7.1 Design and Validation Improvements . . . 25
8.7.2 Future Research Directions . . . 26

9 Conclusion **27**

References **28**

A Measurement Protocol **30**
A.1 Preparation . . . 30
A.2 Calibration . . . 30
A.3 Measurement Procedure . . . 30
A.4 Data Processing . . . 31
A.5 Outcome Measures . . . 31

B Literature Review **32**

Nomenclature

Abbreviations

Abbreviation	Definition
ABS	Acrylonitrile Butadiene Styrene
Add	Adductor Pollicis
AOL	Anterior Oblique Ligament
APB	Abductor Pollicis Brevis
APL	Abductor Pollicis Longus
CT	Computed Tomography
DCL	Dorsocentral Ligament
DRL	Dorsoradial Ligament
EPB	Extensor Pollicis Brevis
EPL	Extensor Pollicis Longus
FDM	Fused Deposition Modeling
FPB	Flexor Pollicis Brevis
FPL	Flexor Pollicis Longus
IML	Intermetacarpal Ligament
MC1, MC2	1^{st} Metacarpal, 2^{nd} Metacarpal
OA	Osteoarthritis
Opp	Opponens Pollicis
PETG	Polyethylene Terephthalate Glycol
PLA	Polylactic Acid
POL	Posterior Oblique Ligament
ROM	Range of Motion
SLA	Stereolithography
TJA	Total Joint Arthroplasty
TMC	Trapeziometacarpal
UCL	Ulnar Collateral Ligament

1 Introduction

1.1. Background

The trapeziometacarpal (TMC) joint is one of the most influential joints in the human body, enabling thumb opposition. This motion is essential for pinch grip and grasping, which is required for many routine tasks, such as turning a key or opening a jar. The joint's saddle shape allows for this complex hand dexterity, but its location on the radial aspect of the wrist offers little bony support [1]. To stabilise the joint over its wide range of motion (ROM), it relies on a complex ligamentous structure. However, there is little consensus in the literature regarding the exact composition and importance of these ligaments. Studies report the involvement of as few as four ligaments [2] to as many as 16 ligaments [1]. More recent studies offer varying accounts of ligament composition [3, 4, 5].

This uncertainty also extends to total joint arthroplasty (TJA), a treatment for TMC joint osteoarthritis in which the affected joint is partially or fully replaced by a prosthesis. During the procedure, certain ligaments must be dissected, yet it remains unclear whether their reattachment improves prosthesis stability or increases the risk of dislocation [6, 7, 8]. These uncertainties highlight the need for systematic investigation of ligament contributions to TMC joint stability.

1.2. State of the Art

Van Ooijen [9] developed an anthropomorphic model of the middle finger, integrating previously designed finger segments and a tendon-ligament system capable of simulating realistic finger motion. The bones were 3D printed, and the ligaments and tendons were simulated using Dyneema rope. Building on this work, Ul Haq [10] created a musculoskeletal model of the finger and investigated the role of lateral bands during dynamic flexion. While these studies advanced the understanding of the finger, no equivalent physical model currently exists for the TMC joint.

1.3. Problem Statement

Despite the first anatomical descriptions of the TMC joint ligaments dating back to Weitbrecht in 1742, their biomechanical role remains incompletely understood. While recent cadaveric studies suggest that the dorsoradial ligament plays a more crucial role in joint stability than the traditionally emphasized anterior oblique ligament (AOL), there is still no consensus on the exact composition or mechanical contribution of the ligamentous structures. For instance, some studies report separate superficial and deep AOL components, while others identify only one. Similar disagreements exist regarding the presence of distinct volar and dorsal intermetacarpal ligaments and the existence of a separate dorsocentral ligament.

These anatomical uncertainties also impact TJA. A scoping review of the literature (Appendix B) found that most studies on trapeziometacarpal prosthesis instability focus on bony morphology (73%), while only a minority (36%) address the influence of ligaments. Moreover, the existing body of research primarily consists of case series and expert opinions (evidence level 4 and 5), highlighting a critical lack of high-quality comparative studies. While implant designs such as the dual mobility prosthesis show promise in reducing dislocation rates, long-term outcomes remain unknown.

There is a clear gap in understanding how periarticular ligaments influence prosthesis stability, particularly following capsuloligamentous dissection and repair during surgery. Addressing this gap could improve implant survival and functional outcomes. Therefore, further research is needed to systematically evaluate the biomechanical role of ligaments in TMC joint stability and their impact on prosthesis behaviour.

1.4. Aim of the Study

The aim of this thesis is to develop a physical model of the TMC joint to investigate the influence of ligaments on joint stability. The model can also serve as a platform to investigate how different ligament configurations and surgical procedures, such as capsular release, affect the stability of TMC prostheses.

2

Anatomy

2.1. Skeletal Structure

To provide a clear and consistent description of thumb motion and anatomical structures throughout this report, anatomical conventions of the hand are used. These include terms to describe the position of anatomical structures with respect to each other (Figure 2.1). The bony anatomy of the hand is shown in Figure 2.2. The TMC joint—the articulation between the trapezium and the first metacarpal (MC1)—has a saddle shape. This saddle shape allows for high mobility but provides less morphologic stability compared to hinge joints (e.g. knee) or a ball-socket joints (e.g. hip).

In addition to the MC1, the trapezium also articulates with the scaphoid, trapezoid, and second metacarpal. The trapezium has little bone support due to its location on the radial aspect of the wrist, since there is no bone on that side. In addition, the articular surface of the TMC joint offers little to no resistance to (sub)luxation. The joint articular surfaces are covered with cartilage to ensure smooth motion. This layer naturally degrades with time, but trauma can speed this up. This process is called osteoarthritis and leads to pain, stiffness, and reduced ROM. A common treatment option is total joint arthroplasty, in which the joint is replaced with a prosthetic implant.

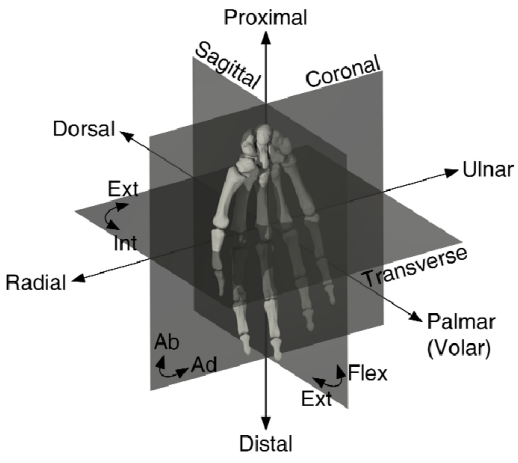

Figure 2.1: Anatomical conventions for the hand. From [11]

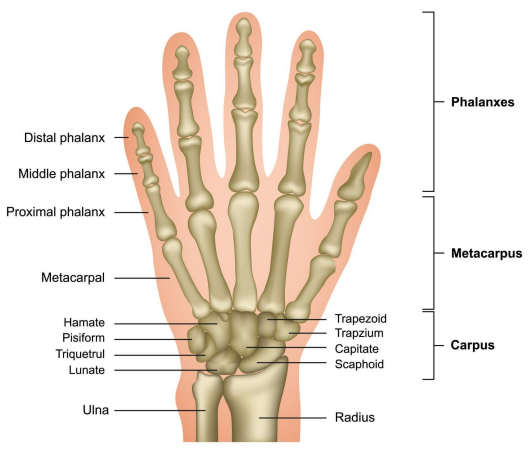

Figure 2.2: Bony anatomy of the right hand. From [12]

2.2. Ligaments

A complex structure of ligaments keeps both the trapezium and metacarpal in place, while also allowing for the wide range of motion required to oppose the thumb. Figure 2.3 shows the ligamentous structures of the hand. Although all ligaments contribute to the stability of the TMC joint to some extent, some are considered the main stabilisers. These main stabilising ligaments are described below.

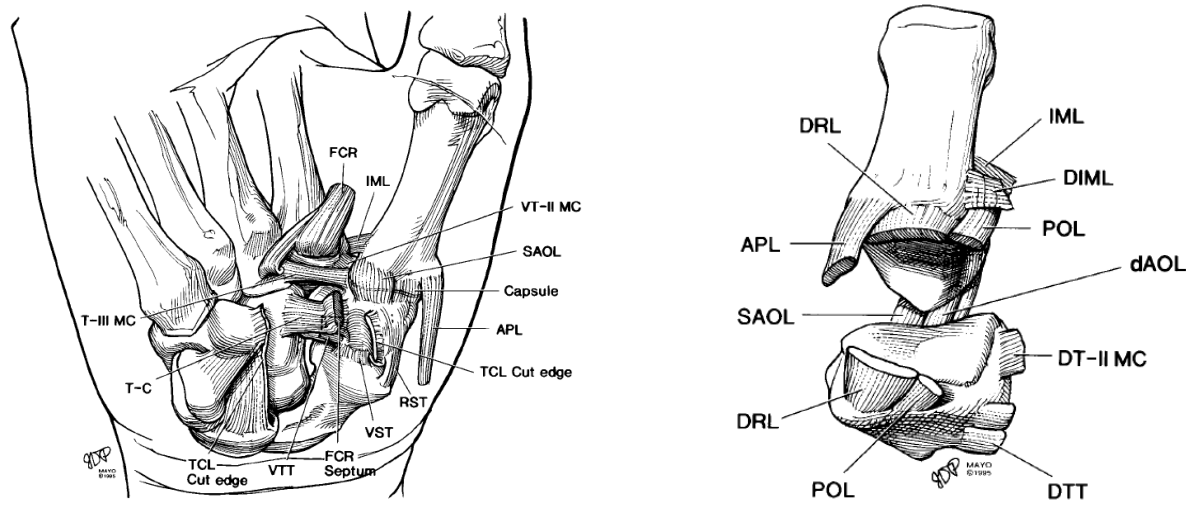

(a) Volar view **(b)** Dorsal view

Figure 2.3: Ligamentous structures of the right hand. From [1].
APL: abductor pollicis longus; dAOL: deep anterior oblique ligament; DIML: dorsal intermetacarpal ligament; DRL: dorsoradial ligament; DT-II MC: dorsal trapezio-second metacarpal ligament; DTT: dorsal trapeziotrapezoid ligament; FCR: flexor carpi radialis; IML: intermetacarpal ligament; POL: posterior oblique ligament; RST: radial scaphotrapezial; SAOL: superficial anterior oblique ligament; T-C: trapezio-capitate; T-III MC: trapezio-third metacarpal; TCL: transverse carpal ligament; VST: volar scaphotrapezial; VTT: volar trapeziotrapezoid; VT-II MC: volar trapezio-second metacarpal.

Anterior Oblique Ligament
The anterior oblique Ligament (AOL) is a capsular ligament that originates from the volar edge of the trapezium and inserts onto the volar edge of the MC1 base. It becomes taut at the extremes of rotation—pronation in particular—and in joint extension and abduction. In some studies a superficial and deep structure was delineated and considered two distinct ligaments [1]. In the literature, the deep AOL is sometimes referred to as the beak ligament. However, more recent studies could not prove the existence of two separate structures [3, 4].

Dorsoradial Ligament
The dorsoradial ligament (DRL) is a capsular ligament that originates from the radial aspect of the dorsal tubercle of the trapezium and inserts onto the dorsoradial edge of the MC1 base. It tightens in supination, regardless of joint position, and also in pronation when the TMC joint is concomitantly flexed. The DRL has also occasionally been called the radial collateral ligament.

Dorsocentral Ligament
The dorsocentral ligament (DCL) is a capsular ligament that originates from the centre of the dorsal tubercle of the trapezium and inserts onto the central dorsal edge of the MC1 base. It was first described by Ladd et al. [3] as being part of the Deltoid Ligament Complex. However, d'Agostino et al. [4] did not observe a distinct DCL. They reported that the DRL appeared to be a continuous sheet on the dorsoradial side.

Posterior Oblique Ligament
The posterior oblique ligament (POL) is a capsular ligament that originates from the ulnar side of the dorsal tubercle of the trapezium and inserts onto the dorso-ulnar edge of the MC1 base. It becomes taut in abduction, opposition, and supination. Together with the DCL and DRL, it forms a fan-shaped structure on the dorsal aspect of the TMC joint, collectively referred to as the *Deltoid Ligament Complex*. In some descriptions, the POL is also referred to as the dorsal oblique ligament.

Intermetacarpal Ligament
The intermetacarpal ligament (IML) is an extracapsular ligament that originates from the dorsoradial side of the second metacarpal (MC2) and inserts onto the volar ulnar MC1. It becomes taut at the

extremes of adduction and stabilises the MC1 during radial translation of its base. Some studies found distinct volar and dorsal IMLs, while more recent studies found only one ligament between the MC1 and MC2.

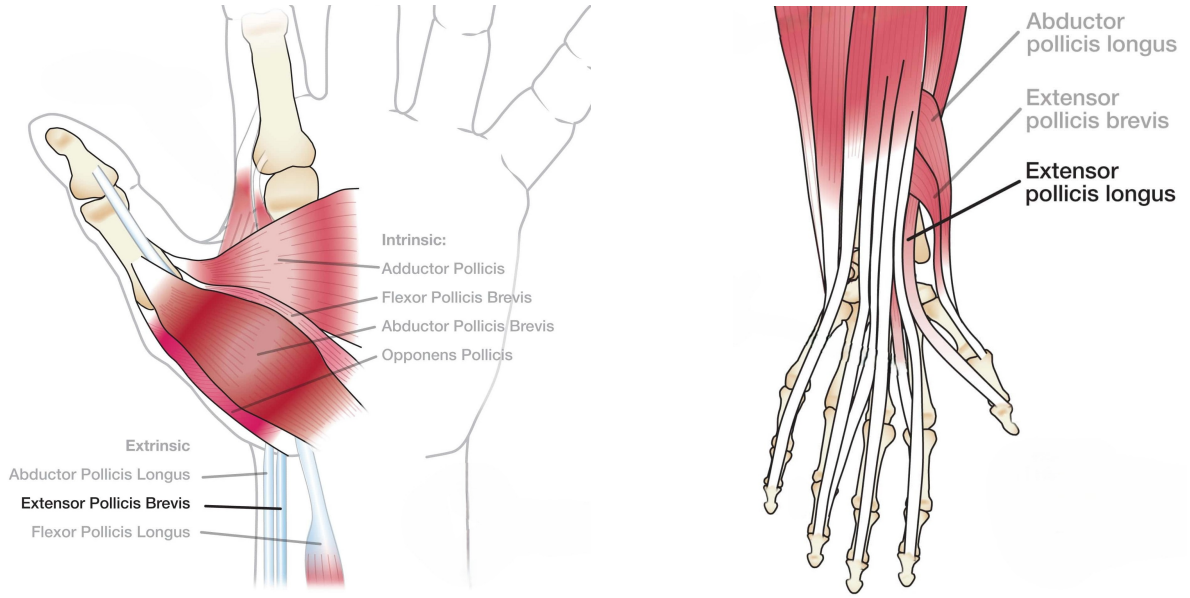

(a) Volar view of left hand

(b) Palmar view of right hand

Figure 2.4: Volar and dorsal views of the thenar muscles. Adapted from [13]

2.3. Muscles and Tendons

The complex motions of the thumb are achieved by multiple muscles that work in concert. Tendons, a strong fibrous tissue, connect muscles to bone. These tendons transmit the force from the muscle to the bone, causing movement. The muscles of the thumb, also called thenar muscles, are shown in Figure 2.4, which can be categorised as intrinsic and extrinsic, the former originating within the hand and the latter originating from outside of the hand. In the case of extrinsic muscles, the tendons run through the thumb to actuate the movements. Table 2.1 lists the thenar muscles and their function.

Muscles and tendons exhibit anatomical variation—naturally occurring differences in tissue structure and organisation between individuals. Some tendons might have different or multiple attachment points or multiple slips [14, 15, 16]. Small changes in muscle insertion points can significantly alter leverage. Anatomical variation could lead to a difference in joint kinematics between individuals, making it difficult to create a universal joint model that is applicable to everyone.

Table 2.1: Thenar muscles and their function

Muscle	Abbr.	Function
Abductor pollicis brevis	APB	Abduction and flexion of MC1
Abductor pollicis longus	APL	Extension and supination of the TMC joint
Adductor pollicis	Add	Adduction of MC1
Extensor pollicis brevis	EPB	Extension and supination of the TMC joint
Extensor pollicis longus	EPL	Extension, adduction and supination of the TMC joint
Flexor pollicis brevis	FPB	Flexion of MC1 and thumb pronation
Flexor pollicis longus	FPL	No clear function in TMC joint motion
Opponens pollicis	Opp	Flexion and pronation of MC1

3 Design

3.1. Design Process

The TMC joint model was developed based on prior work involving a physical model of the middle finger. Due to the anatomical and functional differences of the TMC joint, the model had to be developed from the ground up. However, several concepts from the middle finger model were adapted and, where necessary, modified or improved to suit the TMC joint. As in the previous study, CT data of the relevant bone structure was available and used in designing the bone geometry.

The design process began with the formulation of design criteria, followed by the identification of the relevant soft tissue anatomy. Using the CT data, the geometry of the trapezium and MC1 bones was reconstructed. Alternatives to concepts from the middle finger model were explored and evaluated against the design criteria. The concepts from the middle finger, or their refined versions, were integrated into the design. Rapid prototyping was used iteratively to optimise the design.

3.2. Design Criteria

Due to the complex anatomy of the TMC joint, anatomical accuracy is essential; small deviations can significantly affect joint kinematics. However, given the large number of tendons and ligaments involved in TMC motion and stability, certain anatomical simplifications are necessary to keep the scope of this thesis feasible. The following design criteria aim to strike a balance between anatomical fidelity and practical simplification:

- **Morphology:** The complex shape of the TMC joints articular surfaces plays a key role in its motion and stability. Preserving this morphology in the model is crucial to ensure realistic joint kinematics.
- **Variability:** The precise attachment locations and lengths of ligaments and tendons are not well established. Therefore, the model should allow for adjustable ligament and tendon attachment points.
- **Scale:** Because of the small physical size of the TMC joint, the model should be scaled up to allow space for adjustability. However, increasing the scale also increases the moment arms and, consequently, the joint forces and friction; this must be taken into account.
- **Weight:** Component weight influence the forces acting on the joint and contributes to friction. Model parts should be as lightweight as possible, while still being strong enough to withstand forces generated during use.

3.3. Identification of Relevant Ligaments and Tendons

As mentioned in Section 3.2, the number of ligaments and tendons contributing to the motion and stability of the TMC joint is too large for complete inclusion in the model. A reduction to a manageable and functionally relevant subset is therefore necessary.

The literature reveals substantial variability in the reported number of stabilising ligaments. Bettinger et al. [1] identified 16 stabilising ligaments, whereas Van Brenk et al. [2] listed only four. Among

the most consistently mentioned ligaments are the AOL, DRL, DCL, POL, IML, and the ulnar collateral ligament (UCL). All of these connect to the base of MC1. In contrast, the additional ligaments described by Bettinger et al. mainly stabilise from trapezium cantilever bending and are not included here.

To align with recent anatomical insights, the model simplifies the AOL and IML to single ligaments, as several studies did not distinguish between superficial and deep components of the AOL [3, 4, 5], nor between volar and dorsal components of the IML [3, 5]. The UCL, which originates from the transverse carpal ligament—a structure difficult to replicate—was excluded.

In terms of tendons, the goal is to include the minimum number needed to reproduce the six pure TMC joint motions: flexion-extension, abduction-adduction, and pronation-supination. These combine to produce opposition, the complex motion that allows the thumb to touch the fingertips.

Table 3.1: MC1 motions and their involved muscles

MC1 motion	Involved muscles
Pronation	Opp, FPB
Supination	APL, EPB, EPL
Flexion	Opp, FPB, APB
Extension	APL, EPB, EPL
Abduction	APB
Adduction	Add, EPL

Note: see Table 2.1 for full names.

Table 3.1 lists the muscles responsible for each of these motions. Full names and function of the individual muscles are listed in Table 2.1. The APB, uniquely responsible for abduction, is indispensable. The EPL is involved in three motions and is thus another key candidate. Finally, both the Opp and the FPB can generate flexion and pronation. However, since the FPBs attachment points closely resemble those of the APB—already included in the model—the Opp is chosen for its distinct orientation. As a result, the model includes the following soft tissue structures:

- **Ligaments:** AOL, DRL, DCL, POL, and IML
- **Tendons:** APB, EPL, and Opp

3.4. Rope Attachment

In previous work, ropes were fixated using bolts: the rope was placed in a guide beneath a bolt, and tightening the bolt clamped the rope between the bolt head and the guide. The first version used threaded 3D-printed holes, which were later improved in a second version by replacing these with slotted nuts for greater durability. To further improve the attachment method and reduce wear on the rope, several alternative mechanisms for adjustable fixation were explored:

- **Tuning peg:** Used in string instruments to tension strings by adjusting their length.
- **Cam cleat:** Common in sailing; spring-loaded cams grip the rope in one direction and release it in the other.
- **Ratchet:** A mechanical device that allows unidirectional rotation; some versions permit reversal, like in socket wrenches.
- **Tensioner:** Used in tent or tarp ropes to adjust length and tension.

However, due to the small scale of the model, none of these alternatives proved feasible. While the bolt-and-nut approach remained viable, it still had a drawback: rotating the bolt during tightening could damage the rope. To address this, it was proposed to clamp the rope under the bolt head rather than the tip. This minimises rotational contact with the rope, thereby reducing damage, while remaining suitable for the models compact size.

An additional idea involved placing a layer of material, connected to the model with compliant hinges, between the rope and the bolt to prevent fraying. However, compliant mechanisms require a certain minimum thickness (typically at least twice the printers line width), which is not compatible with the model's scale. They are also prone to wear after repeated use.

Ultimately, clamping the rope under the bolt head was selected as the most practical option. The working principle is illustrated in Figure 3.1.

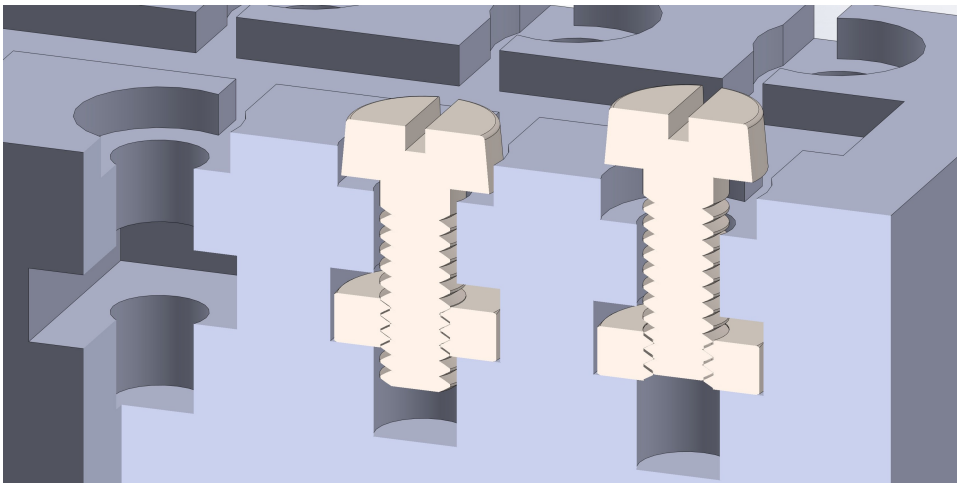

Figure 3.1: Rope attachment system. Tightening the bolt clamps the rope beneath the bolt head while the nut is locked in the slot.

3.5. Bone Model

3.5.1. Obtaining Bone Geometry

To construct the bone model, CT data from a previous study were used. These scans were obtained using a 4D CT scanner (Aquilion One; Canon Medical Systems, Otawara, Japan) to capture the motion of the TMC joint. The output was processed into STL files using IntelliSpace Portal (Philips, Amsterdam, the Netherlands) with the Soft tissue standard kernel. This setting preserves the cartilage layer, which is important for maintaining realistic joint kinematics, as cartilage thickness varies across the articular surface [17]. We assume that the omission of this layer might substantially alter the kinematics of the joint.

The scan data includes the metacarpal and carpal bones, as well as portions of the radius and ulna (see Figure 3.2). Meshmixer (Autodesk Inc., San Francisco, California, USA), a 3D modelling software, was used to isolate the bony structures needed for the model. Since the IML attaches to the MC2, part of it has been fused to the trapezium model. A portion of the trapezoid bone was added as well for support. In addition, the surface of the bones was smoothed to ensure smooth articulation of the MC1 and trapezium. The MC1 and the trapezium models were saved as separate STL files.

Both STL files are again modified in Meshmixer. First, the model is scaled to 3:1 and then is hollowed out with a wall thickness of 2 mm using the hollow function. The STL files are imported as graphics bodies in Solidworks (Dassault Systèmes Solidworks Corp., Waltham, Massachusetts, USA). Each STL produces two bodies; one with the outer surface and one with the inner surface. The graphics bodies are converted to mesh bodies. Now, the bodies can be subtracted from each other to produce a hollow structure. The next subsections describe how the CAD model is built from these hollowed out MC1 and trapezium, respectively.

3.5.2. MC1

The volar aspect of the shaft is cut to make room for rope attachment. A loft is created to facilitate the attachment of the opponens tendon. In the middle, a block is added on which the ropes are fixed. This is done using bolts and nuts, as described in section 3.4. Slots are created in which the nuts are inserted.

On either side of the block a structure similar to a bitt for mooring ships is added. The rope is

Figure 3.2: Raw STL of the hand scan including soft tissue

looped around before being secured to the block. This reduces the stress on the rope attachment and thus the chance of the rope coming undone. Grooves guide the looped rope and prevent slippage during actuation.

Finally, holes are added at the approximate locations of the ligament and tendon attachment sites. This is where the rope enters the bone before it is attached on the inside. Multiple holes per attachment site allow for variability of the attachment. The CAD model is shown in Figure 3.3.

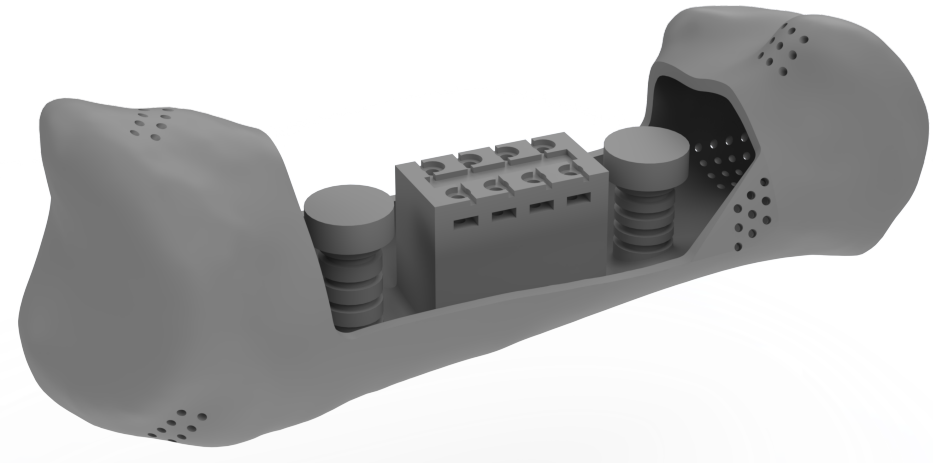

Figure 3.3: CAD model of the MC1, showing rope attachment block, loop structures for load reduction, and variable attachment sites.

3.5.3. Trapezium

The bottom of the trapezium structure is removed, and a base plate is added to support the model. Several additional openings are created to improve access to the interior. As with the MC1, rope entry

holes are added near the anatomical ligament attachment sites, along with a rotated attachment block aligned with the direction of these ligaments.

Figure 3.4: Trapezium CAD model shown from different angles.

The tendons are actuated using levers positioned outside the bone model. Since the APB and opponens are intrinsic muscles—located entirely within the hand—their ropes must pass through the trapezium at anatomically correct attachment sites. Corresponding holes are added for this purpose. A guiding pin mounted on the underside of the base plate redirects the ropes toward the external actuation levers. See Figure 3.4 for the CAD model of the trapezium. The complete assembly of the bone parts is shown in Figure 3.5.

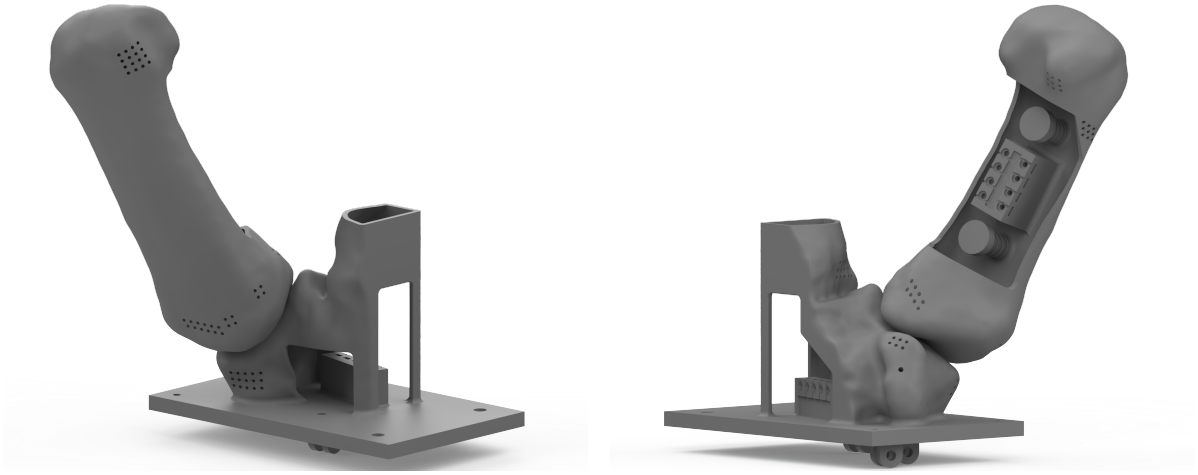

Figure 3.5: Assembly of the bone CAD models shown from different angles.

4

3D Printing

4.1. 3D Printing Method

Given the complex geometry of the TMC joint, the bone model is manufactured through 3D printing. This method was chosen for its short production time, low cost for small production runs, and ability to create complex organic shapes. Two types of 3D printing technology were available: fused deposition modeling (FDM) and stereolithography (SLA). Their key characteristics are compared in Table 4.1.

FDM offers advantages such as faster print speed, lower cost, and ease of use. Post-processing is minimal, typically limited to support removal and surface finishing. SLA, on the other hand, provides high resolution and a smooth surface finish, making it well-suited for small and highly detailed parts.

Although FDM has lower resolution than SLA, the the bone model's relatively large size ensures sufficient detail to reproduce the complex TMC articular surfaces. Any roughness can be smoothed afterwards to reduce friction between the articular surfaces. For these reasons, FDM was selected for printing the bone model.

Table 4.1: Comparison of FDM and SLA 3D printer characteristics

Characteristic	**FDM**	**SLA**
Technology	Melted plastic extruded from a nozzle	Liquid resin cured using a laser
Materials	Thermoplastics	Photosensitive resins
Print speed	Faster	Slower
Resolution	Lower	Higher
Surface finish	Rougher	Smoother
Post-processing	Support removal and surface finishing	Cleaning and post-curing required
Cost	Lower	Higher
Ease of use	Easier	More complex

4.2. Material

Several materials can be used for FDM printing, each with its own advantages and drawbacks. The relevant characteristics of polylactic acid (PLA), acrylonitrile butadiene styrene (ABS), polyethylene terephthalate glycol (PETG) and nylon are summarised in Table 4.2.

Since bone has very low flexibility, the material for the bone model should also be low in flexibility. This rules out nylon, which is very flexible, and PETG, which is medium in flexibility. That leaves PLA and ABS as the most suitable options.

ABS has higher strength, impact resistance, heat resistance, and durability compared to PLA. However, it is more difficult to print, has a lower print speed, and is more prone to warping. PLA, on the

other hand, offers medium strength and durability but is very easy to print, with high print speeds and minimal warping.

Given the scale of the model and the need for rapid prototyping during the design process, PLA is chosen as the material for 3D printing the bone model. While it sacrifices some strength and resistance properties compared to ABS, its ease of use and speed outweigh these drawbacks for this application.

Table 4.2: Comparison of FDM printing material characteristics

Characteristic	**PLA**	**ABS**	**PETG**	**Nylon**
Flexibility	Low	Low	Medium	Very high
Strength	Medium	High	Medium-High	Very high
Impact resistance	Low	High	High	Very high
Heat resistance	Low	High	Medium	High
Durability	Medium	High	High	Very high
Print speed	High	Low	Medium	Low
Ease of use	Very high	Medium	High	Low

4.3. Post-Processing

After printing, support removal and surface smoothing are required. Supports can be removed manually using pliers and cutters, but it becomes challenging when the supports are located in hard-to-reach areas, as is the case with the bone model. Printing supports in a water-soluble material, such as polyvinyl alcohol (PVA), can make removal in such areas easier. However, this requires a dual-extrusion printer and dissolving the supports can take up to a day. Moreover, the available dual-extrusion printer has a much slower print speed—around five times slower than the regular printer—so the latter was used instead.

Once supports are removed, the articular surfaces are smoothed to reduce friction between moving parts. This is done by sanding with progressively finer grits of sandpaper, starting with 800 and ending with 3000 ($800 \rightarrow 1000 \rightarrow 1200 \rightarrow 1500 \rightarrow 2000 \rightarrow 2500 \rightarrow 3000$). Since the print was already produced at a low layer height, sanding could start at a relatively fine grit.

5 Assembly

5.1. Frame Construction

A frame was built using modular 30 mm x 30 mm aluminium construction profiles. On one side of the frame, the 3D-printed trapezium and metacarpal model were mounted, while the actuation system was attached to the opposite side (Figure 5.1). Brackets were added to fix the frame to the table and minimise noise during measurements.

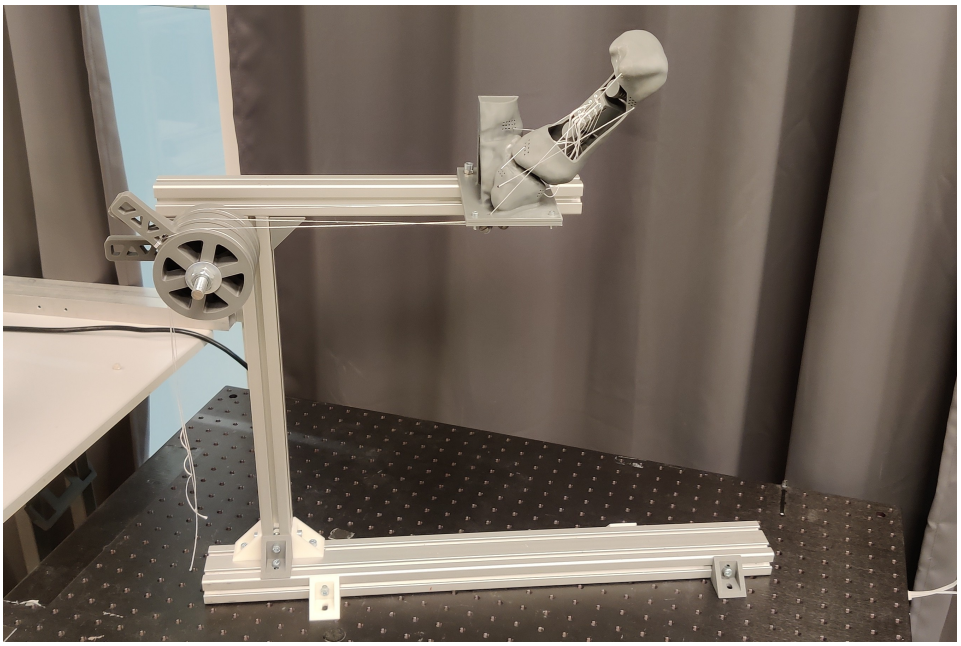

Figure 5.1: Overview of the complete TMC joint model setup, including frame, bone model, and actuation system.

5.2. Ligament Routing

The ligaments of the physical model were represented by Dyneema rope. One end of each rope was threaded through a hole near the approximate attachment site on the trapezium and fixed in place. From there, the rope was routed to its corresponding attachment site on MC1 (Figure 5.2). Ligament length was approximated using values from the literature (Ladd et al. [3]) and scaled to match the 3:1 scale ratio of the model. Since ligament length and attachment sites are subject to anatomical variation, adjustments to the ligament configuration were made until a desirable TMC joint motion was achieved.

Figure 5.2: Frame assembly with the 3D-printed trapezium and metacarpal model mounted in place.

5.3. Tendon Actuation

The tendons were also modelled using Dyneema rope, which was routed through attachment holes at the MC1 insertion sites. The ropes were connected to external levers mounted on the frame, allowing active actuation of thumb motion (Figure 5.3). To guide the tendons in the correct direction, pins were added beneath the base plate. This ensured smooth tendon routing and prevented unwanted friction or misalignment during motion.

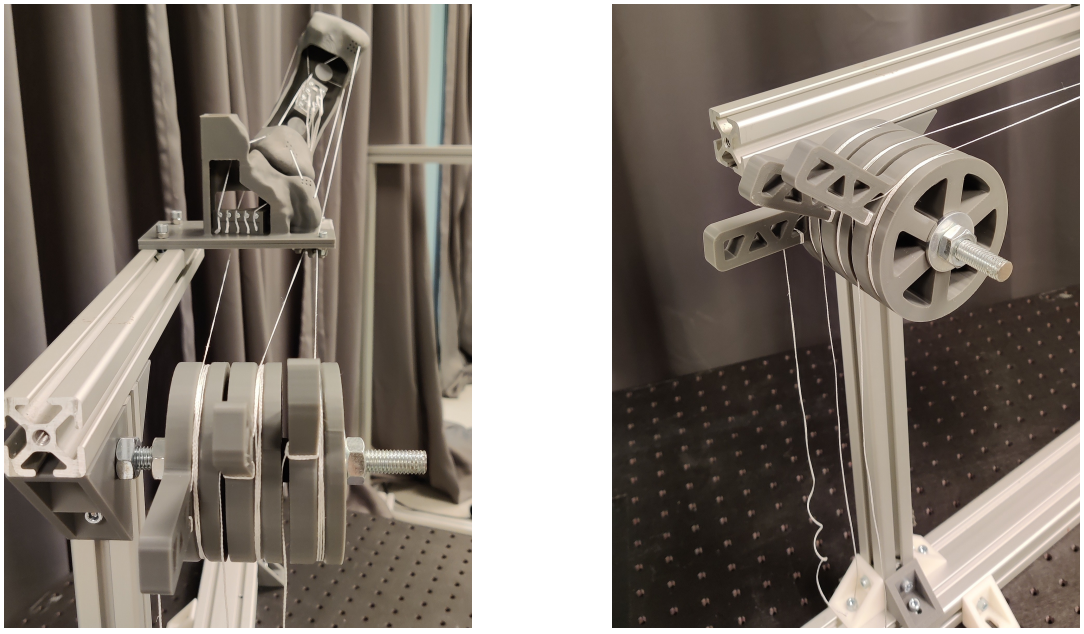

Figure 5.3: Lever-based actuation system for joint motion control.

6 Validation

6.1. Introduction

To verify that the physical model of the TMC joint is an accurate representation of the natural TMC joint, measurements on the motion of the physical model were performed. The aim of these measurements was to determine the ROM of the physical model of the TMC joint. These were compared with the 4D CT data of the TMC joint of the same person on whom the physical model is based. Using the data of the same person for both the design and validation of the physical model minimises the influence of anatomical variation, and hence is assumed to give more reliable results.

6.2. Measurement Protocol

To evaluate the ROM of the physical TMC joint model, motion capture measurements were performed using an OptiTrack (NaturalPoint, Inc., Corvallis, Oregon, USA) motion capture system with Prime^{x} 13 cameras. The model, representing the trapezium and MC1, was mounted on a rigid frame secured to a table to minimise movement artefacts. Retroreflective markers with a diameter of 6.4 mm were placed on both MC1 and the trapezium, ensuring that at least three markers per rigid body were visible at all times.

Figure 6.1: Camera setup for the motion capture trials

Six cameras were positioned around the setup (Figure 6.1) to provide top-down coverage, operating at a sampling frequency of 120 Hz and a resolution of 1.3 megapixel. Calibration was performed using a CW-500 calibration wand (position B configuration), resulting in a Mean Ray Error of 0.240 mm, classified as “excellent” per OptiTrack guidelines [18].

During the measurement trials, rigid bodies for the trapezium and MC1 were defined in Motive software (Figure 6.2). The pivot point of the trapezium rigid body was set to the contact point between trapezium and MC1 in resting position, and the MC1 pivot was aligned to this point to establish a common coordinate system. Trials were performed using both active and passive actuation, and movements measured included flexion-extension, adduction-abduction, and circumduction, with circumduction trials lasting 30 s and flexion-extension and adduction-abduction trials lasting 15 s. For all trials, the first 300 frames were removed during preprocessing to eliminate skewed data from the initiation of motion.

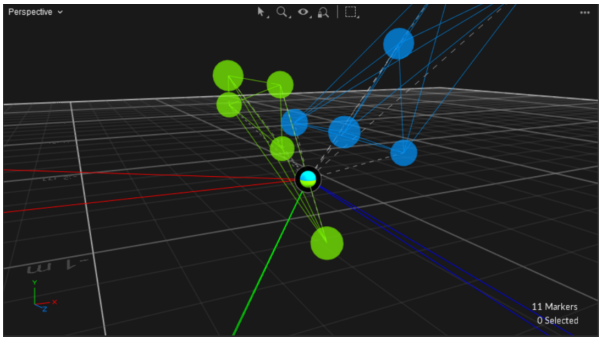

Figure 6.2: Screen capture from Motive showing the rigid bodies and their pivots. Red: x-axis, green: y-axis, blue: z-axis. NB: The pose is slightly off from the resting position in this capture

Motion capture data were exported from Motive as quaternions and converted to rotation matrices for analysis. The relative motion of MC1 with respect to the trapezium was calculated, and Euler angles were extracted using a ZYX intrinsic rotation sequence to determine ROM in each degree of freedom (Figure 6.3). For a detailed, step-by-step description of the measurement protocol, refer to Appendix A.

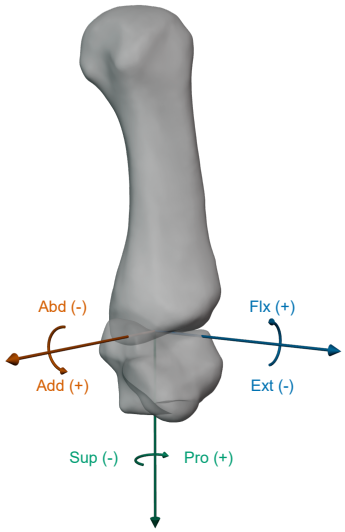

Figure 6.3: Trapeziometacarpal joint with rotational axes and degrees of freedom indicated.

6.3. Data Analysis

The ROM of the model was determined for each measurement. First, the quaternions were converted to rotation matrices. The relative rotation, the rotation of MC1 with respect to the trapezium, was calculated as:

$$\mathbf{R}_{\text{rel}} = \mathbf{R}_{\text{trap}}^{\top}\mathbf{R}_{\text{MC1}}$$

where $\mathbf{R}_{\text{rel}}$ is the rotation of MC1 relative to the trapezium, $\mathbf{R}_{\text{trap}}$ is the rotation of the trapezium relative to the global coordinate system, and $\mathbf{R}_{\text{MC1}}$ is the rotation of MC1 relative to the global coordinate system.

The relative rotation matrix $\mathbf{R}_{\text{rel}}$ is defined as:

$$\mathbf{R}_{\text{rel}} = \begin{bmatrix} r_{11} & r_{12} & r_{13} \\ r_{21} & r_{22} & r_{23} \\ r_{31} & r_{32} & r_{33} \end{bmatrix}$$

Using the method proposed by Cheze et al. [19], the joint angles were extracted from $\mathbf{R}_{\text{rel}}$ using a ZYX intrinsic rotation sequence as follows:

$$\theta_{\text{FE}} = \arctan 2\,(r_{21},\ r_{11}) \qquad \text{(Flexion-Extension)}$$

$$\theta_{\text{AA}} = \arctan 2\,(r_{32},\ r_{33}) \qquad \text{(Adduction-Abduction)}$$

$$\theta_{\text{PS}} = \arcsin\,(-r_{31}) \qquad \text{(Pronation-Supination)}$$

The ROM for each motion was calculated as the difference between the maximum and minimum values of the corresponding joint angle:

$$\text{ROM} = \max(\theta) - \min(\theta)$$

The ROM of the model was compared to the ROM that was extracted from 4D CT data of in-vivo circumduction. These data were obtained from the same subject on which the bone model was based. The data were provided in the form of homogeneous transformation matrices of MC1, one for each capture frame of the 4D CT scan. The homogeneous transformation matrix has the following form:

$$\begin{bmatrix} r_{11} & r_{12} & r_{13} & t_1 \\ r_{21} & r_{22} & r_{23} & t_2 \\ r_{31} & r_{32} & r_{33} & t_3 \\ 0 & 0 & 0 & 1 \end{bmatrix}$$

where the upper-left 3×3 block $\mathbf{R}$ represents the rotation matrix, the rightmost column $\mathbf{t} = [t_1, t_2, t_3]^{\text{T}}$ is the translation vector, and the bottom row [0 0 0 1] ensures the homogeneous form.

The ROM of the TMC joint during in-vivo circumduction during the 4D CT scan was calculated from this rotation matrix in the same way as the for the measurement data. These values were compared to evaluate the accuracy of the model. To visualise MC1 motion during circumduction, the bone was represented as a bar extending distally from the origin of its local coordinate system. The trajectories were then compared with the in-vivo results.

7

Results

7.1. Actively Actuated Motion

The model was actively actuated during a series of measurements involving three distinct motion types: circumduction, flexion-extension, and adduction-abduction. For each motion type, three trials were performed. The resulting rotation angles of MC1 relative to the trapezium are presented in Figure 7.1. Each row corresponds to a specific motion type and includes three sub-figures, one for each trial. In every sub-figure, the MC1 rotation around its three anatomical axes—flexion-extension, adduction-abduction, and pronation-supination—is plotted in the colour corresponding to those in Figure 6.3.

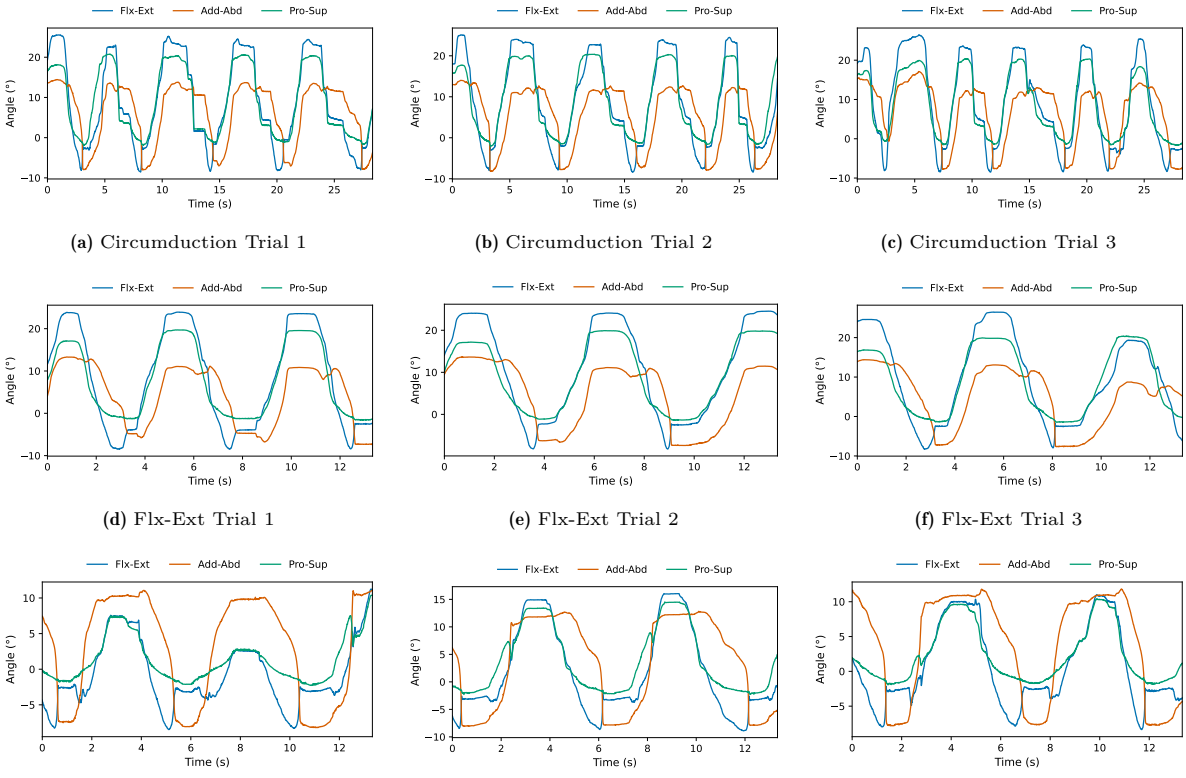

(a) Circumduction Trial 1 **(b)** Circumduction Trial 2 **(c)** Circumduction Trial 3

(d) Flx-Ext Trial 1 **(e)** Flx-Ext Trial 2 **(f)** Flx-Ext Trial 3

(g) Add-Abd Trial 1 **(h)** Add-Abd Trial 2 **(i)** Add-Abd Trial 3

Figure 7.1: MC1 rotation during actively actuated circumduction (top row), flexion-extension (middle row), and adduction-abduction (bottom row).

For all three motions and across all individual trials, flexion-extension and pronation-supination are coupled, as can be deferred from the similarities in amplitude and phase. In the trials for circumduction

and pure flexion-extension, the amplitude of the adduction-abduction angle is smaller than those for flexion-extension and pronation-supination. During all trials for pure adduction-abduction, an abrupt flexion motion is noticeable at the extremes of abduction.

7.2. Passively Actuated Motion

To evaluate the performance of the actuation system, the same set of measurements was repeated using passive actuation. In this case, the MC1 was manually moved by hand rather than using the system's levers. The resulting rotation angles of MC1 relative to the trapezium are shown in Figure 7.2. As before, each motion type is represented in a dedicated row, with three sub-figures corresponding to individual trials. The rotation around the three anatomical axes—flexion-extension, adduction-abduction, and pronation-supination—is plotted in each sub-figure.

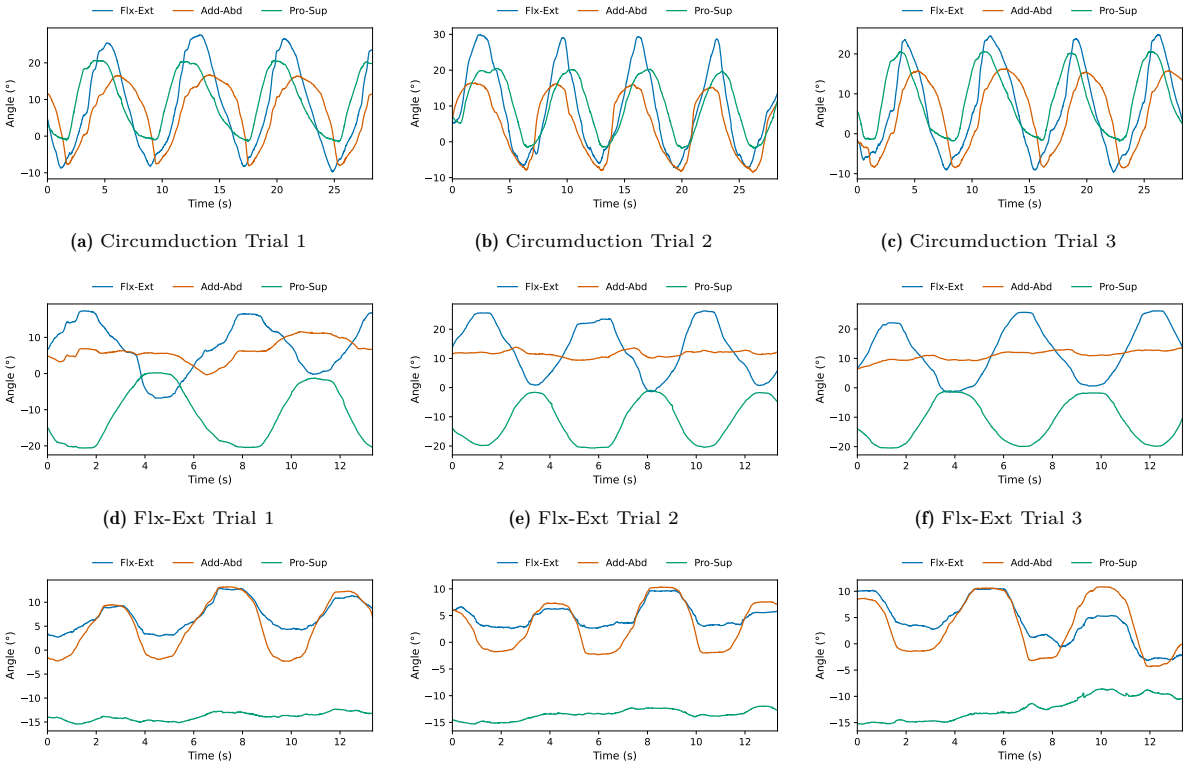

(a) Circumduction Trial 1 **(b)** Circumduction Trial 2 **(c)** Circumduction Trial 3

(d) Flx-Ext Trial 1 **(e)** Flx-Ext Trial 2 **(f)** Flx-Ext Trial 3

(g) Add-Abd Trial 1 **(h)** Add-Abd Trial 2 **(i)** Add-Abd Trial 3

Figure 7.2: MC1 rotation during passively actuated circumduction (top row), flexion-extension (middle row), and adduction-abduction (bottom row).

Across all trials for circumduction and pure flexion-extension, similar to the trials with active actuation, flexion-extension and pronation-supination are coupled. Additionally, during all trials for pure flexion-extension, a negative correlation can be seen between adduction-abduction and flexion-extension. During pure adduction-abduction motion, flexion-extension and adduction-abduction are coupled across all trials and the pronation-supination is close to constant.

7.3. Range of Motion

The ROMs of the joint model are presented in Table 7.1. Results for each motion type are grouped. The mean and standard deviation for each set of trials is provided to assess inter-trial consistency. The standard deviation is relatively low, except for the passive adduction-abduction and flexion-extension trials. For the actively actuated trials, circumduction and flexion-extension show less variability than adduction-abduction.

The ROM of the TMC joint from the in-vivo 4D CT scan is shown in Table 7.2 together with the mean values of the ROMs of the model during actively and passively actuated circumduction. Active

Table 7.1: Range of Motion for the thumb movements for each trial, including their mean ± standard deviation

DoF	**Trial 1** (°)	**Trial 2** (°)	**Trial 3** (°)	**Mean ± SD** (°)
Active circumduction				
Flx-Ext	34.12	33.48	34.93	34.18 ± 0.59
Add-Abd	22.45	22.23	24.90	23.19 ± 1.21
Pro-Sup	22.74	22.45	22.11	22.43 ± 0.26
Active flexion-extension				
Flx-Ext	32.43	32.80	34.79	33.34 ± 1.04
Add-Abd	20.70	21.06	22.09	21.28 ± 0.59
Pro-Sup	21.32	21.33	21.91	21.52 ± 0.27
Active adduction-abduction				
Flx-Ext	19.74	24.95	19.38	21.36 ± 2.54
Add-Abd	19.27	20.90	19.65	19.94 ± 0.69
Pro-Sup	12.67	16.79	12.40	13.95 ± 2.01
Passive circumduction				
Flx-Ext	37.43	37.23	34.37	36.34 ± 1.40
Add-Abd	24.80	24.88	24.85	24.85 ± 0.03
Pro-Sup	22.22	22.24	22.50	22.32 ± 0.13
Passive flexion-extension				
Flx-Ext	24.16	27.70	27.67	26.51 ± 1.66
Add-Abd	11.94	4.50	7.06	7.83 ± 3.09
Pro-Sup	20.82	19.78	19.44	20.01 ± 0.59
Passive adduction-abduction				
Flx-Ext	10.17	7.21	13.75	10.38 ± 2.68
Add-Abd	15.54	12.71	15.17	14.47 ± 1.25
Pro-Sup	3.11	3.35	6.72	4.40 ± 1.65

and passive circumduction show similar ROM. When compared to the physical model, the ROM of the TMC joint during the in-vivo experiment is 1.83 times as high for flexion-extension, 2.21 times as high for adduction-abduction, and 1.64 times as high for pronation-supination. Figure 7.3 shows MC1 rotation during the in-vivo experiment. Flexion-extension and pronation-supination are coupled and there is a negative correlation with abduction-adduction.

Table 7.2: Range of Motion (ROM) in degrees for Euler angles during circumduction.

	Flx-Ext (°)	**Add-Abd (°)**	**Pro-Sup (°)**
Active circumduction	34.18 ± 0.59	23.19 ± 1.21	22.43 ± 0.26
Passive circumduction	36.34 ± 1.40	24.85 ± 0.03	22.32 ± 0.13
In-vivo 4D CT	66.66	54.86	36.53

Note: Model-based ROMs (active and passive) are reported as mean ± standard deviation across simulation trials. The in-vivo 4D CT values represent a single-subject measurement without variability.

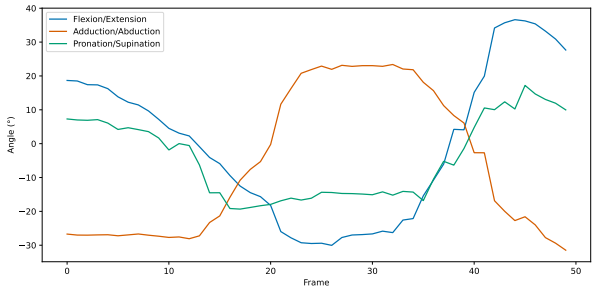

Figure 7.3: MC1 rotation during in-vivo circumduction experiment

The ROM of the TMC joint model is visualised in Figure 7.4. A 145 mm bar extends from the origin of the MC1 local coordinate system (blue dots) along its y-axis in the distal direction, with the tip marked by an orange dot. Compared to the in-vivo results from Yuan (Figure 7.5), the general shape of the cone is similar, but the cone from the in-vivo study is wider. Furthermore, the MC1 base shows noticeable translation in the proximal-distal direction, and waist of the shape is visible in the ulnar view in stead of the palmar view.

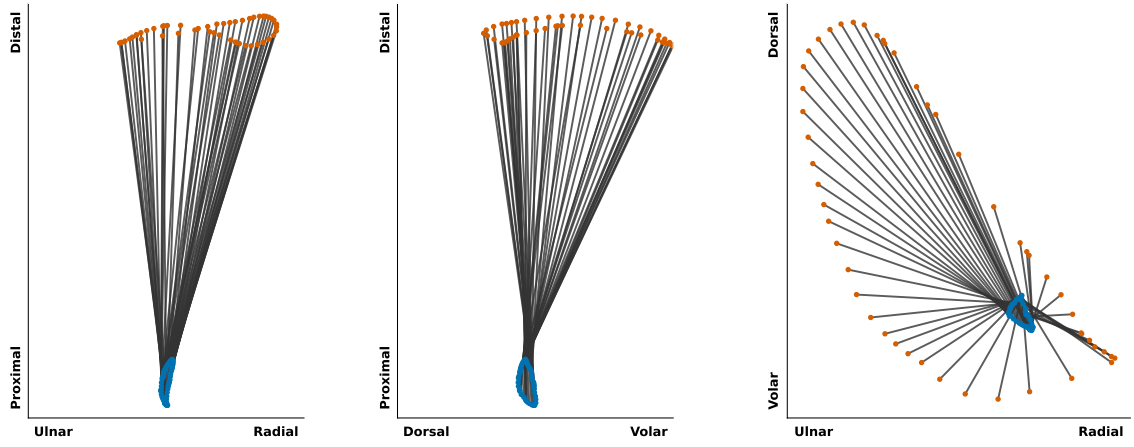

(a) Volar view **(b)** Ulnar view **(c)** Top-down view

Figure 7.4: Different views of the motion locus of the MC1 during the first passive circumduction trial. Blue dots: MC1 base. Orange dots: MC1 head

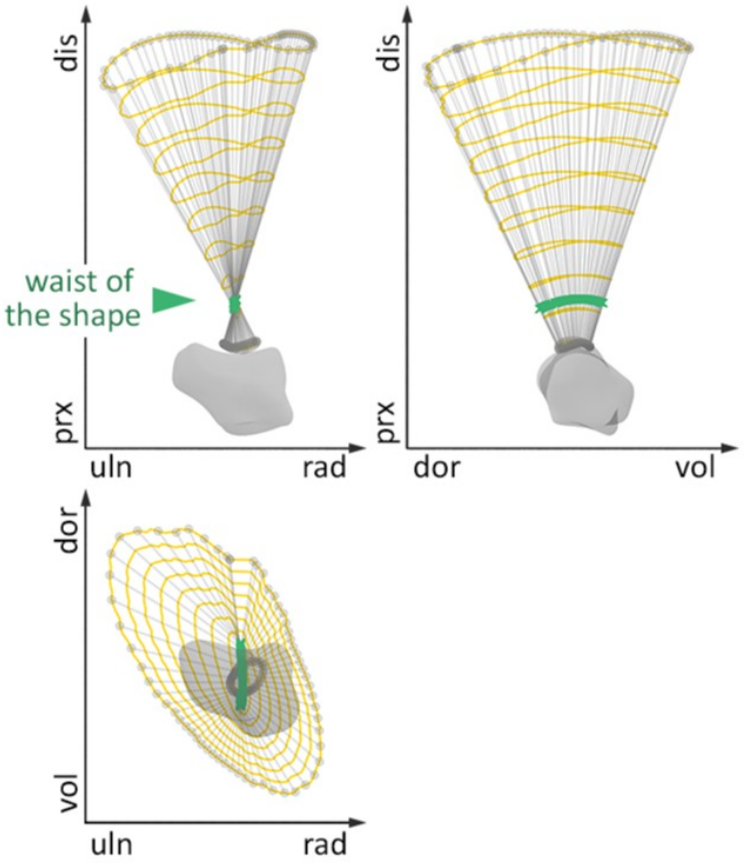

Figure 7.5: Mean motion locus of the MC1 from the in-vivo study. From [20] *Note:* This is the mean of all participants from the in-vivo study.

8

Discussion

8.1. Summary of Key Findings

The aim of this thesis was to develop a physical model of the trapeziometacarpal (TMC) joint that can be used to investigate the influence of ligaments on joint stability. Simulation results of joint motion using both active and passive actuation demonstrated that the range of motion (ROM) of the model is inconsistent with the ROM derived from the in-vivo 4D CT data, especially for flexion-extension and adduction-abduction. Comparison of the simulation results for active and passive actuation show consistent ROM for circumduction, but differences in ROM for the two pure motions—flexion-extension and adduction-abduction.

8.2. Model Performance Compared to In-Vivo Motion

8.2.1. Coordinate System Alignment

A primary factor contributing to the discrepancy in ROM between the physical model and the in-vivo data is the potential misalignment of coordinate systems used during motion capture. The local coordinate system—the pivot point of the trapezium rigid body—had to be manually set in the right place and orientation in Motive. The only available landmarks for proper alignment were the markers, no visualisation of the bone outline was available. Extra markers were placed on the model to improve alignment, but the number of extra markers was severely limited by available space. Not only was the articular surface inaccessible due to the presence of the first metacarpal (MC1), sufficient distance between the markers had to be kept to prevent overlap on the camera view, and hence potential loss of marker data.

8.2.2. Subject-Specific Anatomy

A secondary but still important factor is anatomical variability, which likely contributed to the observed differences in joint motion. Bone geometry was extracted from the CT data and used in the design of the physical model. However, the composition of the ligamentous structure of the subject was unknown. Ligament length, origin point, and insertion point vary between people. These metrics influence joint kinematics, a slight deviation could result in a considerable change in joint ROM. Although variability of ligament length and attachment points to the bone were incorporated in the design of the model, it seems that the combinations of ligament length and attachment points were incorrect during the joint motion simulations.

8.3. Model Simplifications and Their Implications

8.3.1. Ligament Selection

The most critical simplification in the model was the choice of which ligaments to include. The number of ligaments influencing TMC joint stability reported in the literature varies between four and 16 [1, 2]. To make the project manageable, a subset of five ligaments was selected that span the TMC joint. The ulnar collateral ligament (UCL) was omitted because it originates from the transverse carpal ligament,

a structure that is difficult to incorporate into the physical model. The remaining ligaments were chosen based on their consistent description in the literature and their functional relevance to joint stability.

Earlier anatomical studies described distinct volar and dorsal intermetacarpal ligaments (IMLs) [1, 21], whereas more recent work supports the presence of a single continuous band [3, 5]. The model reflects this updated view by including one IML, which plays an important role in lateral stability and in limiting excessive axial motion. Its presence may also have contributed to the observed coupling between flexion-extension and pronation-supination. However, by omitting discrete dorsal and volar components, the model may not fully capture the rotational constraints of the native joint.

8.3.2. Uniform Stiffness

A further simplification was that each ligament was represented by a single strand of Dyneema rope, resulting in uniform stiffness across all ligaments. In-vivo, ligaments differ in width, thickness, and material properties, which influence their stiffness. A comparison between the dimensions reported by Bettinger et al. [1] and their follow-up study on material properties [22] suggests that thicker ligaments exhibit greater stiffness. This finding is supported by D'Agostino et al. [4], who observed similar trends when comparing the anatomical and mechanical characteristics of the dorsoradial ligament (DRL) and anterior oblique ligament (AOL). By neglecting stiffness variability, the model likely under-represents the contribution of stiffer ligaments and overemphasises the role of more compliant ones. This simplification has a notable impact on the joints dynamic response, particularly in motions where ligament stiffness varies with direction and position.

8.3.3. Simplified Fibre Architecture and Attachments

A further effect of the single-strand representation is the reduction of ligaments to simple point-to-point attachments. While this has a more modest influence than stiffness, it still limits the ability of the model to capture the complex fibre architecture that contributes to realistic joint stability. Native ligaments consist of multiple fibre bundles that span a broader attachment area and engage progressively during motion. This fibre recruitment leads to direction-dependent tensioning, with different bundles taking load depending on joint configuration [23]. In addition, load sharing among collagen fibres, as demonstrated in tendon fascicles, shows that fibres act collectively rather than independently to bear mechanical load [24]. Reducing the ligament to a single strand with fixed-point attachments prevents these behaviours from being represented in the model, potentially oversimplifying how ligaments interact with bone and contribute to joint stability. This may particularly affect coupled motions like pronation-supination during circumduction, where small changes in force direction are critical for accurate joint behaviour.

8.4. Evaluation of the Actuation System

The effectiveness of the actuation system was assessed by simulating thumb motion using both active and passive control. During circumduction, both methods produced similar motion paths and ROMs, indicating that the system permits movement through the full extent of the joint's capabilities. However, the motion path during active actuation appeared jagged—particularly at the extremes of flexion-extension and adduction-abduction—suggesting limited smoothness in transitions between movement directions.

In contrast, actively actuated flexion-extension showed a smoother trajectory, with noticeable irregularities only at the extremes of extension and adduction. This pattern suggests that the actuation system struggles to execute adduction-abduction smoothly, particularly at full extension. The limitations are most pronounced in the isolated adduction-abduction trials, where a steep slope in the adduction angle highlights a lack of controlled, gradual motion. These findings strongly suggest that adduction is not adequately simulated by the current actuation setup.

The physical model was initially designed with the hypothesis that three tendons would be sufficient to produce the full ROM, assuming that the extensor pollicis longus (EPL) could facilitate both extension and adduction. The results clearly indicate that this assumption was incorrect, and that a dedicated tendon is necessary to accurately simulate adduction.

8.5. Comparison to Existing Models

To date, no physical model of the TMC joint has been reported in the literature. This thesis presents, to the best of the author's knowledge, the first physical simulation of the TMC joint, aimed at investigating the role of ligaments in thumb stability. While virtual models of the TMC joint exist and continue to advance [25], these lack the tangible, hands-on interactivity provided by a physical model.

Despite the novelty of this work, the approach builds on earlier studies, particularly the physical finger model developed by Van Ooijen [9]. That model featured 3D-printed bones and Dyneema rope ligaments and tendons, offering a modular platform for studying finger biomechanics. The present study adopts the same material choices, but the TMC joint introduces additional anatomical and mechanical complexities.

Whereas the finger joints primarily generate planar (2D) motion, the TMC joint moves in three-dimensional space, with coupled motions that require more sophisticated ligament placement and actuation strategies. This added complexity affects both mechanical design and control. By extending principles of physical modelling from the finger to the thumb, this study establishes a new foundation for future work on more realistic TMC joint models.

8.6. Limitations

8.6.1. General Limitations

A key limitation of this study is the reliance on data from a single subject. While using matched bone geometry and joint kinematics from the same individual enhances internal consistency—since identical bone morphology should result in comparable motion patterns—this approach limits the generalisability of the findings. Anatomical and biomechanical variability across the population means that results may not be broadly representative. Further investigation involving a wider range of anatomical specimens is needed to assess inter-subject variability and its implications for model robustness.

Despite common challenges in optical motion capture—such as marker occlusion and tracking loss—this study benefitted from a well-calibrated system and optimal marker placement. As a result, rigid body motion data were recorded without gaps, ensuring continuous and reliable kinematic tracking throughout all motion trials.

8.6.2. Design and Validation Limits

Several limitations emerged from the physical model design and validation process. First, the absence of anatomical imaging in the motion capture workflow made it difficult to precisely align local coordinate systems to anatomical landmarks. As a result, uncertainty in the orientation of the trapezium's coordinate system may have contributed to discrepancies between simulated and in-vivo kinematics.

Second, the physical model was constructed based solely on bone geometry, without subject-specific data on soft tissue properties. This incomplete anatomical representation limits the models ability to fully replicate the functional constraints of the native joint.

Finally, several model simplifications—as previously discussed—likely contributed to deviations in joint mechanics. These include the omission of the UCL, the simplified representation of ligaments as single strands with uniform stiffness, and the use of only three tendons for actuation. While necessary for feasibility, these design choices reduce the fidelity of the model in replicating the complex relationship between ligaments and joint motion.

8.7. Recommendations

8.7.1. Design and Validation Improvements

Based on the limitations identified in this study, several improvements are recommended to enhance the fidelity and functionality of the physical TMC joint model.

First, additional ligaments could be included to better replicate anatomical reality. Incorporating the UCL, despite the challenge of modelling its origin on the transverse carpal ligament, may significantly improve model accuracy. Likewise, representing both a volar and dorsal IML could provide new insights into the IMLs role in joint stability, especially in light of recent anatomical studies reporting the presence of a single IML.

Second, the use of subject-specific soft tissue data, in addition to bone geometry, could enhance the precision of ligament placement and improve the anatomical fidelity of the model.

Third, modelling ligaments with multiple strands of rope could allow for ligament-specific stiffness and enable more realistic load-sharing between fibres, improving the biomechanical behaviour of the system.

Crucially, a fourth tendon should be added for actuation. The current model's reliance on the extensor EPL to produce both extension and adduction results in an unrealistic motion pattern. Introducing the adductor pollicis tendon could resolve this issue and allow for more anatomically accurate thumb movements.

Finally, to improve validation accuracy during motion capture, the use of anatomical imaging is recommended for more reliable definition of local coordinate systems, particularly when aligning them to bone landmarks.

8.7.2. Future Research Directions

Beyond improving the current model, future research should focus on applying and extending it to address broader questions of thumb biomechanics.

First, a multi-subject comparison would help to account for inter-individual anatomical variability. Such work could clarify how differences in bone morphology and ligamentous structures influence joint kinematics and stability, thereby improving the generalisability of findings.

Second, the model could be integrated with computational simulations, such as finite element or musculoskeletal models. This hybrid approach would allow cross-validation of results.

Finally, the model offers potential as a platform for testing surgical techniques and prosthesis designs. Future studies could adapt it for evaluating implant stability or for educational and pre-operative planning purposes.

9

Conclusion

The aim of this thesis was to develop and validate a physical model of the trapeziometacarpal (TMC) joint in order to study the role of ligaments in thumb stability. The model was constructed on a 3:1 scale using 3D-printed bones and Dyneema rope ligaments, and its kinematics were compared against in-vivo data derived from 4D CT.

The model successfully reproduced circumduction motion, but its range of motion—especially for flexion-extension and adduction-abduction—was lower compared to the in-vivo results, highlighting the model's current limitations in capturing realistic joint mechanics. Both active and passive actuation produced similar ROM during circumduction, but differed for isolated motions—especially adduction. Expanding the actuation system with an extra tendon dedicated to adduction motion could improve the accuracy of the model.

Several factors were identified as sources of the difference between the ROM of the model and the in-vivo data. These include potential misalignment of the local coordinate system during motion capture, subject-specific anatomical variability, and model simplifications. Reducing the number of ligaments and representing them with a single strand of rope reduced model fidelity.

Despite these limitations, this thesis presents the first physical model of the TMC joint. It demonstrates the feasibility of this approach and provides a foundation for further refinement. This model offers the unique possibility of hands-on experimentation for investigating the role of ligaments on joint stability. It could also serve as a platform for prosthesis testing and surgical training.

Future research should focus on improving the model by refining the ligament and tendon representations. Incorporating subject-specific soft tissue data could enhance model fidelity, while multi-subject comparison could improve the generalisability of findings. Integrating the physical model with computational simulations would allow cross-validation of results.

In summary, this thesis provides a novel step toward physical modelling of the TMC joint. While current limitations constrain its anatomical accuracy, it lays the foundation for further research and clinical application in thumb biomechanics.

References

[1] P.C. Bettinger et al. “An Anatomic Study of the Stabilizing Ligaments of the Trapezium and Trapeziometacarpal Joint”. In: *The Journal of Hand Surgery* 24.4 (1999), pp. 786–798.

[2] B. Van Brenk et al. “A Biomechanical Assessment of Ligaments Preventing Dorsoradial Subluxation of the Trapeziometacarpal Joint”. In: *The Journal of Hand Surgery* 23.4 (1998), pp. 607–611.

[3] A.L. Ladd, J. Lee, and E. Hagert. “Macroscopic and microscopic analysis of the thumb carpometacarpal ligaments”. In: *Journal of Bone and Joint Surgery* 94.16 (2012), pp. 1468–1477.

[4] P. D’Agostino et al. “Comparison of the anatomical dimensions and mechanical properties of the dorsoradial andăanterior oblique ligaments of the trapeziometacarpal joint”. In: *The Journal of Hand Surgery* 39.6 (2014), pp. 1098–1107.

[5] M. Esplugas et al. “Trapeziometacarpal ligaments biomechanical study: Implications in arthroscopy”. In: *Journal of Wrist Surgery* 5.4 (2016), pp. 277–283.

[6] A. Andrzejewski and P. Ledoux. “Maïa trapeziometacarpal joint arthroplasty: Survival and clinical outcomes at 5 years follow-up”. In: *Hand Surgery and Rehabilitation* 38.3 (2019), pp. 169–173.

[7] A. Brauns, P. Caekebeke, and J. Duerinckx. “The effect of cup orientation on stability of trapeziometacarpal total joint arthroplasty: a biomechanical cadaver study”. In: *Journal of Hand Surgery (European Volume)* 44.7 (2019), pp. 708–713.

[8] B. Van Hove et al. “Trapeziometacarpal total joint arthroplasty: The effect of capsular release on range of motion”. In: *Hand Surgery and Rehabilitation* 39.5 (2020), pp. 413–416.

[9] J. van Ooijen. “Humanising robot fingers: Design, prototyping, and validation of an anthropomorphic robot finger with humanoid joint-ligament systems, tendon configurations and supporting ligaments”. MA thesis. Delft University of Technology, 2022.

[10] R.S. Ul Haq. “Development and Verification of an Anthropomorphic Mechanical Finger Model in OpenSim”. MA thesis. Delft University of Technology, 2024.

[11] I.M. Bullock, J. Borras, and A.M. Dollar. “Assessing Assumptions in Kinematic Hand Models: A Review”. In: *proceedings of the 2012 4th IEEE RAS & EMBS International Conference on Biomedical Robotics and Biomechatronics (BioRob)*. Rome, Italy, June 2012, pp. 139–146.

[12] The White House Clinic. *Anatomy, Pathology and Treatment of the Wrist & Hand*. 2024. URL: `https://www.whitehouse-clinic.co.uk/articles-and-advice/anatomy-pathology-and-treatment-of-the-wrist-hand` (visited on 06/19/2025).

[13] American Society for Surgery of the Hand. *Body Anatomy: Upper Extremity Muscles*. 2025. URL: `https://www.assh.org/handcare/safety/muscles` (visited on 06/19/2025).

[14] G.A. Abdel-Hamid, R.A. El-Beshbishy, and I.H. Abdel Aal. “Anatomical variations of the hand extensors”. In: *Folia Morphologica* 72.3 (2013), pp. 249–257.

[15] S. Deivasigamani, A. Azad, and S. Yang. “The Variable Insertional Anatomy of the Abductor Pollicis Longus: Functional Relevance and Relationship to Adjacent Thumb Extensors”. In: *Hand* 18.1 (2021), pp. 145–152.

[16] M. Lonne et al. “Clinical Examination of the Extensor Pollicis Brevis: Anatomical Study and Description of a Novel Clinical Sign”. In: *The Journal of Hand Surgery (Asian-Pacific Volume)* 23.3 (2018), pp. 330–335.

[17] B. Dourthe et al. “Assessment of healthy trapeziometacarpal cartilage properties using indentation testing and contrast-enhanced computed tomography”. In: *Clinical Biomechanics* 61 (2019), pp. 181–189.

[18] OptiTrack. *Calibration - Motive Documentation*. Accessed: 2025-06-07. NaturalPoint, Inc. 2023. URL: https://docs.optitrack.com/motive/calibration.

[19] L. Cheze et al. "A joint coordinate system proposal for the study of the trapeziometacarpal joint kinematics". In: *Computer Methods in Biomechanics and Biomedical Engineering* 12.3 (2009), pp. 277–282.

[20] T. Yuan. "Movement of Thumb-Base Joints: In-Vivo anatomy and biomechanics to support Implant Design". Dissertation (TU Delft). Delft University of Technology, 2023. ISBN: 978-94-6366-766-1. DOI: 10.4233/uuid:cbe936ed-32a4-4084-ae9d-a8f6a2b36480.

[21] M. Nanno et al. "Three-dimensional analysis of the ligamentous attachments of the first carpometacarpal joint". In: *The Journal of Hand Surgery* 31.7 (2006), pp. 1160–1170.

[22] P.C. Bettinger et al. "Material properties of the trapezial and trapeziometacarpal ligaments". In: *The Journal of Hand Surgery* 25.6 (2000), pp. 1085–1095.

[23] M. Solomonow. "Ligaments: A source of musculoskeletal disorders". In: *Journal of Bodywork and Movement Therapies* 13.2 (2009), pp. 136–154.

[24] S.E. Szczesny and D.M. Elliott. "Interfibrillar shear stress is the loading mechanism of collagen fibrils in tendon". In: *Journal of Orthopaedic Research* 10.6 (2014), pp. 2582–2590.

[25] M. Dong et al. "Using a finite element model of the thumb to study trapeziometacarpal joint contact during Lateral Pinch". In: *Clinical Biomechanics* 101 (2023), p. 105852.

A

Measurement Protocol

A.1. Preparation

Markers:

- Retroreflective markers with a diameter of 6.4 mm were used.
- At least five markers were placed on both the first metacarpal (MC1) and the trapezium, positioned with sufficient spacing to avoid marker overlap in camera views.
- Placement ensured at least three markers per rigid body were visible at all times, the minimum required to define a rigid body.
- Care was taken to avoid interference with the rope actuation system.

Environmental preparation:

- The physical model of the trapeziometacarpal (TMC) joint was mounted onto a rigid frame secured to a table to minimise movement artefacts during measurements (see Figure 6.1).
- Six OptiTrack Prime^{x} 13 cameras (NaturalPoint, Inc., Corvallis, Oregon, USA) were mounted on tripods and arranged around the model.
- Cameras were positioned to provide top-down views, ensuring each marker was captured by at least three cameras simultaneously while avoiding visibility of other cameras in each cameras field of view.
- The camera system operated at a sampling frequency of 120 Hz with a resolution of 1.3 megapixel.
- All reflective surfaces in the capture volume, including nuts and bolts used for rope attachment, were covered with duct tape to minimise extraneous reflections.

A.2. Calibration

The camera system was calibrated using the wanding method, employing a CW-500 calibration wand with the markers in position B configuration. During calibration, the wand was moved throughout the capture volume to enable Motive software to compute camera positions and orientations based on the known geometry of the wand markers. Calibration yielded a Mean Ray Error (MRE) of 0.240 mm, classified as *excellent* (MRE < 0.30 mm) per OptiTrack guidelines [18].

A.3. Measurement Procedure

Rigid body definitions:

- In Motive, rigid bodies for the trapezium and MC1 were created by manually selecting the corresponding markers (see Figure 6.2).
- The pivot point of the trapezium rigid body was translated to the contact point between trapezium and MC1 in resting position.
- The axes were defined as:

  - **x-axis**: volar-dorsal
  - **y-axis**: proximal-distal
  - **z-axis**: radial-ulnar
- The MC1 pivot was aligned with the trapezium pivot to establish a common coordinate system.

Tasks performed:

- *Active actuation trials*: thumb motion simulated using tendon actuation.
- *Passive actuation trials*: MC1 moved manually through its ROM without tendon use.
- *Movements measured*:
  - Flexion-extension
  - Adduction-abduction
  - Circumduction (combination of flexion-extension and adduction-abduction)

Trial durations:

- Circumduction trials: 30 s each
- Flexion-extension and adduction-abduction trials: 15 s each

Data preprocessing:

- For all trials, the first 300 frames were removed to eliminate skewed data resulting from the initiation of motion.

Recording validation:

- Motion data were inspected for missing marker data to ensure reliability before export.

A.4. Data Processing

Motion capture data were exported from Motive as quaternions in CSV format. Quaternions were converted to rotation matrices. The relative rotation of MC1 with respect to the trapezium was calculated using:

$$\mathbf{R}_{\text{rel}} = \mathbf{R}_{\text{trap}}^{\top} \mathbf{R}_{\text{MC1}}$$

where $\mathbf{R}_{\text{rel}}$ is the rotation matrix describing MC1 relative to the trapezium, $\mathbf{R}_{\text{trap}}$ the rotation of the trapezium relative to the global coordinate system, and $\mathbf{R}_{\text{MC1}}$ the rotation of MC1 relative to the global coordinate system.
Euler angles were extracted from $\mathbf{R}_{\text{rel}}$ using a ZYX intrinsic rotation sequence, defined as:

$$\theta_{\text{FE}} = \arctan 2\,(r_{21},\ r_{11}) \qquad \text{(Flexion-Extension)}$$

$$\theta_{\text{AA}} = \arctan 2\,(r_{32},\ r_{33}) \qquad \text{(Adduction-Abduction)}$$

$$\theta_{\text{PS}} = \arcsin\,(-r_{31}) \qquad \text{(Pronation-Supination)}$$

The range of motion (ROM) was calculated for each angle as:

$$ROM = \max(\theta) - \min(\theta)$$

A.5. Outcome Measures

- **Primary outcomes**: ROM of flexion-extension, adduction-abduction, and pronation-supination during both active and passive actuation trials.

B

Literature Review

The Influence of Trapezium Morphology and Ligaments on Trapeziometacarpal Implant Instability: A Scoping Review

D J Esenkbrink

Abstract

Background Several surgical treatment options exist to treat trapeziometacarpal osteoarthritis. Better strength, range of motion and faster convalescence is achieved with replacement arthroplasty compared to soft tissue arthroplasty, but it also has a higher complication rate. **Objective** This scoping review aims to provide an overview of available literature regarding the influence of trapezium morphology and ligaments on trapeziometacarpal implant instability and identify gaps in knowledge. **Design** PubMed and Scopus online databases were searched for articles that report on the influence of trapezium morphology or ligaments on trapeziometacarpal implant instability, of which 22 were selected for data charting. **Results** The majority of the studies (73%) report on the influence of morphology, while 36% report on the influence of ligaments. Case reports are the most frequent (68%) and mostly evidence level 4 and 5 studies were found. **Conclusions** Dual mobility is a promising solution to implant instability, but only short-term results are available due to its novelty in the field of trapeziometacarpal arthroplasty. The influence of periarticular ligaments is affected by bone morphology and the role of ligaments on implant instability is still not fully understood. Further research on the capsuloligamentous structures is necessary, especially comparative studies of higher level of evidence would be beneficial.

Keywords— Trapeziometacarpal, implant, subluxation, loosening

Introduction

The trapeziometacarpal (TMC) joint, also referred to as the thumb carpometacarpal or thumb base joint, is the articulation between the trapezium and the first metacarpal (figures 1 & 2). It has a lot of influence on manual dexterity, being crucial for daily living skills such as grasping objects, pinching and opening jars. In a study by Dahagin et al. [1], 21.2% of women (age $\geq$55 years) were found to have osteoarthritis (OA) in the TMC joint. These results are similar to the prevalence reported by Armstrong et al. [2], who also found that 28% of those affected with TMC OA experience basal thumb pain, increasing to 55% for combined TMC and scaphotrapezial OA. This condition is considered as a major cause of disability in the ageing population. In the early stages of OA, nonoperative treatment is used to reduce pain. When the osteoarthritic TMC joint has deteriorated too much for this to be effective, the focus will shift towards surgical treatment options; these include arthrodesis, trapeziectomy (often in combination with ligament reconstruction and tendon interposition (LRTI) or suspension ligamentoplasty), arthroscopy and prosthetic joint replacement.

Superiority of one of these procedures over the others has not been proven yet [3]. Prosthetic joint replacement seems to have good short-term results with faster recovery [4] and improved strength (mainly pinch grip) and range of motion (ROM) [4, 5]. However, in the long term prostheses have a higher complication and failure rate than non-implant arthroplasty [6]. Ball-and-socket design prostheses are not suitable for TMC replacement arthroplasty according to Wachtl et al. [7] This is because of the way this type of implant changes joint kinematics, especially translations are limited by the spherical design. However, prosthesis designs are still being improved, with the double mobility principle being the newest development. This principle relies on a second articular surface be-

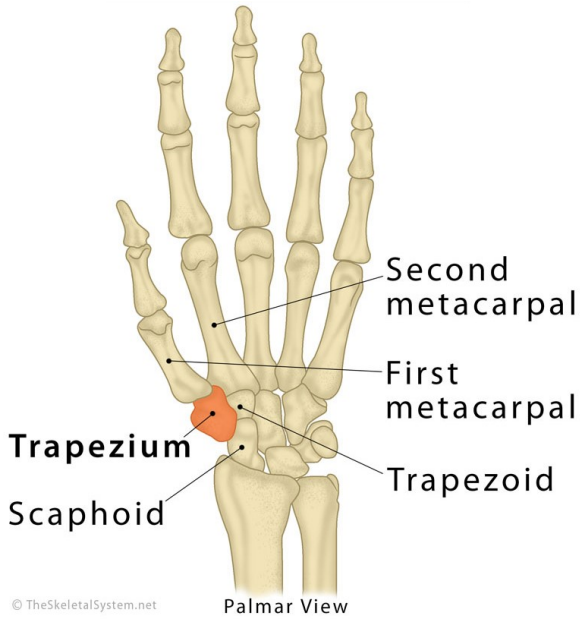

Figure 1: Bony anatomy of the hand showing the trapezium and surrounding bones. From [9]

tween the cup and the polyethylene liner, intended to reduce the dislocation rate. Another factor in implant stability are the periarticular ligaments, but their exact role on implant stability is still unclear [8].

A scoping review was conducted to provide an overview of literature regarding the influence of trapezium morphology and ligaments on trapeziometacarpal implant instability and identify gaps in knowledge in this area. To guide the search, the following two research questions have been formulated:

1. What are the biomechanical causes regarding trapezium morphology leading to TMC implant instability?

2. What influence do ligaments have on TMC implant instability?

The PCC (Population, Concept, Context) framework has been used as a foundation to structure the search strategy. For this review, population is not applicable, since we are not looking at a specific population. We are looking into trapeziometacarpal implant instability, thus we have chosen these three terms as concepts. Within

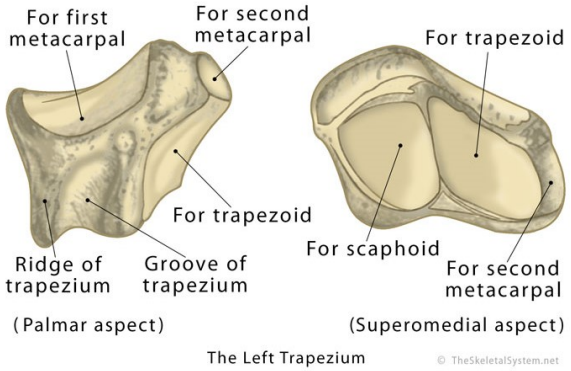

Figure 2: Articular surfaces of the trapezium. From [10]

these concepts, we are investigating the influence of trapezium morphology and ligaments. These will be the context.

Methods

In our review, we included journal articles written in English that report on the influence of trapezium morphology or ligaments on TMC implant instability. Studies that mention influence, but cite this from other studies, are excluded. Case reports with a study population of fewer than 5 cases are excluded. Concerning implant instability, we only included papers that report on implant (sub)luxation or aseptic loosening, because these are the most common modes of implant instability. Note that cup placement is also considered as trapezium morphology, because the cup becomes part of the trapezium and its placement determines the shape of the trapezium.

A combination of search terms based on the concepts of the PCC framework was used. Table 1 shows the keywords and synonyms related to each concept as well as MeSH headings that are relevant to the concept. Boolean operators are used to combine the search terms. The PubMed and Scopus electronic databases were searched for relevant articles up until March 2022. The complete search strategy for both PubMed and Scopus are presented in Appendix A.

After searching both databases, duplicates were removed. The titles and abstracts were screened by two independent reviewers to assess the article

Table 1: Search terms used per concept

Trapeziometacarpal	**Implant**	**Instability**
Trapeziometacarpal [tw]	Implant* [tw]	Instability [tw]
TMC [tw]	Prosthes* [tw]	Unstable [tw]
Carpometacarpal [tw]	Joint replacement [tw]	Sublux* [tw]
CMC [tw]	Arthroplast* [tw]	Dislocat* [tw]
Thumb bas* [tw]	Arthroplasty, replacement, finger [mh]	Displace* [tw]
Thumb metacarpal [tw]	Hemiarthroplasty [mh]	Loosen* [tw]
Carpometacarpal joints [mh]	Joint prosthesis [mh]	Treatment failure [mh]
Trapezium bone [mh]		Prosthesis failure [mh]

tw = text word, mh = MeSH heading

for eligibility using the inclusion criteria. Any disagreements between the reviewers were resolved by discussion and consensus. Of the remaining articles, the full texts were screened only by the author. Potentially relevant articles found in reference lists of the full text articles were also assessed

Data from eligible articles were charted by a single reviewer using a data-charting form. This form was developed by the author and discussed with other reviewers. We extracted data on first author, year of publication, study design, level of evidence, location of study and key findings relevant to our research questions. For case series, population, mean follow-up time and prosthesis type were also recorded. The studies were divided in two groups; studies reporting on the influence of morphology on the stability of TMC implants and studies reporting on the influence of ligaments on the stability of TMC implants. Studies reporting on both were added to both. For both groups, we summarised key findings related to our research questions.

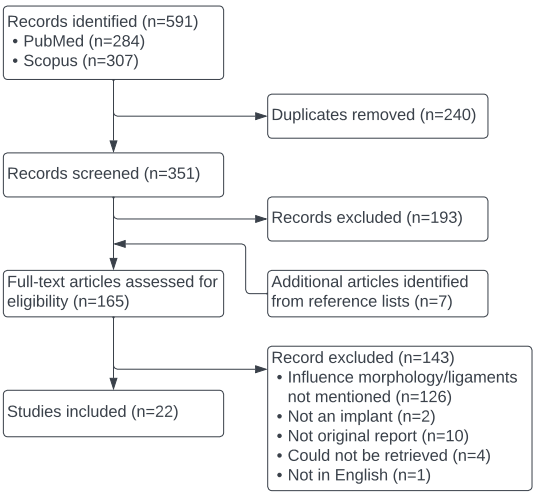

Figure 3: Flow diagram for article selection

Results

Study characteristics

A combined search of the PubMed and Scopus databases yielded a total of 591 results (284 and 307 respectively), of which 351 remained after removal of duplicates. After screening of the title and abstract, 193 articles were excluded. An additional 7 articles were identified through reference scanning, leaving 165 full-text articles to be assessed for eligibility. Of these, 143 were excluded for the following reasons: 126 did not mention the influence of morphology or ligaments, 2 did not report on implants, 10 were not considered original research (i.e. cited relevant findings from other studies), 4 could not be retrieved and 1 did not have a full-text in English. Thus, 22 articles were included. Figure 3 shows a flow diagram of the selection of sources of evidence.

Table 2 shows some study characteristics of the included articles. Almost half of the articles were published between 1991 and 2010 (41%). Most of the studies were conducted in Belgium (23%), France (23%) and the USA (23%). The level of evidence of the included studies is mostly level 4 (73%), no level 1 or 2 studies that met the inclusion criteria were found. Most of the case reports had a population between 20 and 49 patients (40%) and were short-term (73%), no long-term studies met

the inclusion criteria. Note that Wachtl et al. [7] did a case series with two different prostheses, the de la Caffinière and Ledoux prostheses, with different population size and mean follow-up. In the lower part of table 2 it is split into two separate studies, one for each prosthesis. Synthesis of results can be found in appendix B. Key findings relevant to our research questions are discussed in the next sections.

Table 2: Study characteristics

All articles (N=22)		Count (%)
Year of publication		
	1970-1990	3 (14%)
	1991-2010	9 (41%)
	2011-2017	4 (18%)
	2018-2022	6 (27%)
Country		
	Belgium	5 (23%)
	Denmark	2 (9%)
	France	5 (23%)
	Spain	1 (5%)
	Sweden	1 (5%)
	Switzerland	2 (9%)
	UK	1 (5%)
	USA	5 (23%)
Level of evidence		
	1-2	0 (0%)
	3	1 (4%)
	4	16 (73%)
	5	5 (23%)
Case reports (N=15)		Count (%)
Population size		
	5-19	2 (13%)
	20-49	6 (40%)
	50-99	4 (27%)
	≥100	3 (20%)
Mean follow-up (m)		
	Short (<60)	11 (73%)
	Medium (60-119)	4 (27%)
	Long (≥120)	0 (0%)
Implant type		
	Avanta SR TMC	2 (13%)
	CMI	1 (7%)
	Caffinière	1 (7%)
	Elektra	1 (7%)
	Guepar	1 (7%)
	Ledoux	2 (13%)
	Maïa	3 (20%)
	Moje Acamo	1 (7%)
	Pyrocardan	1 (7%)
	Swanson silastic	2 (13%)

Influence of morphology on implant stability

The earliest study reporting on the influence of morphology on implant stability is by Lister et al. [11]. After prosthetic replacement of the trapezium, movements which normally would occur at two carpal joints, occur at the articulation of the implant and scaphoid. This increased ROM increases the risk of subluxation. In a 1996 biomechanical study by Imaeda et al. [12], it was found that the TMC joint has separate axes for flexion-extension and abduction-adduction in the trapezium and the base of the first metacarpal respectively. A ball-and-socket design implant cannot replicate this, because of the fixed centre of rotation. Although it may provide for stronger pinch and grasp, it may also relate to loosening of the trapezial cup. Wachtl et al. [7] also linked the fixed centre of rotation to cup loosening. They indicate that the first metacarpal lies lateral to the trapezium in the normal TMC joint. Prostheses with the axis of the cup collinear to the axis of the stem tend to bring the first metacarpal in a more medial position. This amplifies the already considerable shear forces in the normal TMC joint, which can lead to loosening of mainly the trapezial component. They claim that the ball-and-socket design is not suitable for TMC prostheses. A biomechanical study by Spartacus et al. [13] seems to confirm this. They used CT scans of TMC joints in various postures and CAD models of a ball-and-socked design TMC prosthesis to model the displacement of the prosthesis head relative to the cup. In each posture of each subject, the displacement of the head was greater than that of the cup, i.e. the head numerically penetrated the cup. In vivo this could overstress the prosthesis, which could partly explain the short lifespan of ball-and-socket design TMC prostheses. In a case series on the Pyrodardan spacer, Gerace et al [14] report no cases of implant instabil-

ity and attributes this partly due to the biconcave shape of the implant.

Ledoux [15] Attributes early dislocations to incorrect cup placement (i.e. misalignment w.r.t. trapezium surface, which leads to mechanical impingement between the prosthesis cup and neck) or insufficient resection of a medial osteophyte. When early dislocation occurs despite correct implantation, the dislocation is linked to the small diameter of the head. In this case a double mobility prosthesis is advised, since it has a bigger diameter head. Bricout and Rezzouk [16] found a statistically significant association between incorrect positioning of the cup and both complications (P=0.06) and the need for revision surgery (P<0.001). The surgeon must make sure that the cup is optimally aligned to avoid implant instability. The presence of osteophytes (or lack of osteophyte resection) can cause dislocation due to a cam effect. Pérez-Úbeda et al. [17] also experienced problems with inadequate osteophyte resection, resulting in a 55% (11 out of 20) loosening rate. They found that persistence of a part of the medial osteophyte influenced the radial position of the trapezial component. Slight variations of mainly the radial position of the trapezial component increase the loosening rate and can cause a radial subluxation of the metacarpal. Pendse et al. [18] achieved a lower loosening rate of 18% (11 out of 62) with the same prosthesis, although it is still high. They attribute this difference to the fact that they positioned the trapezial component centrally in the majority of the cases, as opposed to the radial positioning by Pérez-Úbeda et al. To achieve central positioning, the scaphotrapezial joint was exposed to visualise the apex of the trapezium. The trapezial component was aligned in line with this apex.

In a study by Duerinckx and Caekebeke [19], radiographs of healthy participants were used to determine the centre of ROM and identify a landmark that has a fixed relation to this centre. This study suggests that the cup should be placed parallel to the proximal articular surface of the trapezium (PAST) to minimise risk of luxation. In a later case series, Caekebeke and Duerinckx [20] used this PAST to align the prosthesis cup. The cup angle never exceeded more than 10 degrees relative to ideal cup position. Only one subluxation and no dislocations were observed, which was due to excessive bone growth with distalisation of the stem. The authors consider the adequate cup placement as an important factor to the zero dislocation rate. This is confirmed in a cadaveric study by Brauns et al. [8]. They found that incorrect cup placement will cause impingement between the prosthesis neck and cup, which leads to dislocation. Cup placement parallel to the PAST seems to be associated with the lowest risk of dislocation.

Martinez de Aragon et al. [21] encountered a high dislocation rate of 19% (10 out of 54) for the CMI hemiarthroplasty. This is attributed to inadequate preparation of the trapezium cup and backed by the fact that seven of the cases were salvaged by deepening the cup. Centralised placement of the cup was found useful in preventing dorsal subluxation. Klahn et al. [22] had to remove 33% (13 out of 39) of the prostheses due to aseptic loosening. They argued that, because pinch forces at the pulp of the thumb are magnified approximately tenfold, the stresses on the implant increase significantly, increasing the risk of loosening. The ball-and-socket design with a fixed centre of rotation seems to be an important factor in the high stresses on the implant. Even worse results were seen in a study by Hansen and Vainorius [23], who observed progressive osteolysis in 89% (8 out of 9) of the cases during follow-up. There seem to be no problems with a similar implant from the Moje Company used in the first metatarsophalangeal (MTP) joint of the foot, as well as the Acamo-PIP implant used in the proximal interphalangeal (PIP) joint of the hand. Since these implants are made of the same material and are both cementless, the authors suggest that the difference in performance is due to the quality and shape of the bone. The MTP and PIP joints have bones with a hard cortical area compared to the trapezium. Lemoine et al. [24] found a very strong correlation (p<0.0001) between weakening of the lateral cortical bone of the trapezium and onset of cup loosening. Conservation of the lateral walls of the trapezium seems to be an important factor in a stable trapezial fixation.

Influence of ligaments on implant stability

The proximal side of the metacarpal has a lip or "hook" on the ulnar side that projects towards the trapezium, preventing radial subluxation of the metacarpal. This hook effect is lost when the entire trapezium is resected during replacement arthro-

plasty. According to Eiken [25] it is important that ligamentous structures should be reinforced on both the ulnar and volar side to compensate for the loss of this hook effect and thereby decreasing the risk of subluxation. In a case series by Braun [26], the first four cases resulted in subluxation due to inadequate volar ligamentary reconstruction. Of the remaining 11 cases, only one implant subluxed despite reconstruction of the volar ligament. During revision it was found that the volar ligament had completely disappeared.

In a review Linscheid [27] states that if the collateral and accessory collateral ligaments are cut during joint excision, their resistance to subluxation is compromised. Instead of the stresses being transmitted to the cortical bone by the ligaments, the prosthetic components will transmit stresses to the endosteal surface. The intracapsular ligaments also help divert subluxating and out of plane forces from the prosthesis to the ligamentous insertions on the cortical bone. Still, the influence of ligaments on TMC joint stability is not well understood. The same is found by Wachtl and Sennwald [28], who argue that cutting the restraining ligaments, as recommended by Ledoux to increase thumb mobility, increase the already high shear forces on the TMC joint. They state that similar changes occur in osteoarthritis and lead to progressive subluxation. They plead for unconstrained prostheses which retain the ligaments. When implanting the Pyrocardan spacer, Gerace et al. [14] were able to preserve the capsuloligamentous structures due to the small thickness of the implant. Partly due to this, there were no cases of implant instability.

In a case series on the Maïa prosthesis, Andrzejewski and Ledoux [29] found a dislocation rate of 9.7%, of which half occured during the first postoperative week. The dislocation rate is higher than other studies on the same prosthesis as well as other unconstrained prostheses. According to the authors this may be explained by the extensive release of all capsular and ligament attachments in combination with the small prosthetic head. In a biomechanical study, van Hove et al. [30] found that total joint arthroplasty in combination with complete capsular release significantly increases the ROM for flexion-extension. This could lead to early dislocation, especially before capsular healing has occurred.

Brauns et al. [8] argue that due to the reduction to a single centre of rotation, inherent to a ball-and-socket design prosthesis, the dorsal capsuloligamentous structures no longer provide stability to the joint. Instead it creates a dislocating force in the dorsal direction due to tethering of the ligaments. These dislocations might be prevented by performing complete capsular release after total joint arthroplasty.

Discussion

Quality of available literature

The objective of this scoping review was to provide an overview of the literature that report on the influence of trapezium morphology or ligaments on TMC implant instability, and to identify gaps in knowledge in this area. From the study characteristics it becomes clear that there is a lack of high level of evidence research on this topic. No level 1 and 2, and only 1 level 3 study met the inclusion criteria. The majority of the included studies are case series, of which none are long-term and and most have a study population of fewer than 50. Since implant instability develops over time, it is crucial that more long-term studies are available to be better able to assess the factors leading to implant instability.

Influence of morphology on implant stability

Of the 22 included articles, 16 report on the influence of morphology. Half of these report that inadequate cup placement results in a higher risk of cup loosening. Pendse et al. [18] exposed the scaphotrapezial joint to visualise the apex of the trapezium, which was used to align the trapezial component. Pérez-Úbeda et al. [17] encountered a higher loosening rate with the same prosthesis placed more radially. Even though Pendse et al. believe that the trapezial components in their study were placed more centrally due to their method of aligning, subgroup analysis did not show a higher loosening rate for misaligned trapezial components. Duerinckx and Caekebeke [19] developed a different method to adequately align the trapezium cup using the proximal articular surface of the trapezium (PAST). They used this method in a case series of 50 Maïa prostheses and reported no dislocations or loosening at a mean follow-up of 65 months [20].

Due to the small variation in cup angulation with respect to ROM, they could not show that misalignment of the cup leads to more complications.

The incomplete removal of osteophytes is also a factor in TMC implant instability. Osteophytes might induce a cam effect, leading to early dislocation [15,16], or complicate the adequate positioning of the trapezial component [17, 18], increasing the risk of loosening. Lemoine et al. [24] also found that weakening of the lateral wall of the trapezium is correlated with onset of cup loosening. Preservation of the lateral wall of the trapezium seems to be an important factor in TMC implant stability.

From the above it seems that meticulous surgical technique has a considerable influence on TMC implant instability. Not only should attention be paid to the complete removal of osteophytes, the surgeon should also make sure that the implant components, and specifically the trapezial component, are adequately positioned. A few methods have been described to achieve adequate cup alignment, but is has not yet been clearly shown that the implementation of one of these methods actually leads to fewer complications. Further research on methods for adequate cup alignment is necessary to show what method leads to fewer complications.

The change in joint kinematics after total joint arthroplasty with a ball-and-socket implant, i.e. the reduction to a fixed single centre of rotation, is also a factor leading to implant instability. Imaeda et al. [12] and Klahn et al. [22] link this to a higher risk of loosening. Wachtl et al. [7] even states that due to this change in joint kinematics, ball-and-socket implants are not suitable for replacing the TMC joint. However, the development of prostheses based on the dual mobility concept, adopted from hip arthroplasty, might refute this claim. This type of prostheses rely on a second articulation between the shell of the cup and the polyethylene liner. At first, like normal ball-and-socket prostheses, the prosthesis head moves within the liner until the neck comes into contact with the rim of the liner. After this, the second articulation is functional until the neck comes into contact with the rim of the shell. Since this concept is relatively new in TMC arthroplasty, only short-term studies are available. Even though the results are promising, with some studies reporting a 0% dislocation rate [31–34], long-term studies are needed to evaluate the effectiveness of the dual mobility concept.

There seems to be a gap in the literature on anatomically shaped implants and the influence of their anatomical shape on stability. Of the studies included in this review, only 2 reported on an anatomically shaped implant, being the Avanta SR TMC, with disappointing results regarding implant stability [17,18]. The Stablyx Arthroplasty System is an anatomically shaped hemiarthroplasty introduced in 2013. Only one short-term study with 12 patients being followed up to the 24 month mark is available [35] with no cases of loosening, dislocations or instability. Long term studies with a higher population are needed to validate these promising results.

Influence of ligaments on implant stability

With only 7 of the 21 included articles reporting on the influence of ligaments on TMC implant stability, it seems that there are still some unknowns in this area. The contradicting conclusions on whether to cut the periarticular ligaments during joint replacement only underline this. Arguments for cutting the periarticular ligaments are that this improves thumb mobility and prevents tethering of ligaments which results in a dislocating force [8]. However, this increased motion could lead to intraprosthetic impingement and dislocation at the extremes of motion [30]. Cutting the restraining ligaments also increases the forces on the joint [28], partly because subluxating forces are no longer diverted from the prosthesis to the ligamentous insertions on cortical surfaces [27]. This seems to be a problem especially during the first post-operative weeks before capsular scarring increases joint stability [29]. Further research on the short- and long-term effects of capsular release on TMC implant instability is needed.

Limitations

This study has a few limitations. The first is that only articles written in English were included. Quite some articles referred to papers written in French that could have contained valuable information regarding TMC implant instability. Also, only two databases were searched, of which only one is medicine-focused. Another limitation, inherent to the methodology of scoping reviews, is that no critical appraisal of individual sources of evi-

dence has been performed, since the objective is to provide an overview of available literature, not to assess the methodological quality or risk of bias.

Conclusion

The reduction of the saddle joint with an instantaneous centre of rotation to a ball-and-socket joint with a fixed centre of rotation results in increased stresses on the prosthesis and ultimately in loosening of the prosthesis. However, the rise of the dual mobility concept in TMC prostheses, that reduce the stresses on the prosthesis, seem to be a solution to this problem. Long-term results are not yet available, thus it might take some years before the effectiveness of this concept can be evaluated. Inadequate positioning of the trapezial cup is the biggest factor in prosthesis loosening. A few landmarks have been used to properly align the cup, but more studies are required to verify their effectiveness.

The influence of periarticular ligaments on prosthesis stability is still unclear. Some studies report that these ligaments reduce stresses on the prosthesis and should therefore be kept intact to reduce the risk of implant instability. On the other hand some studies suggest that, partly due to the changed joint kinematics, these ligaments induce dislocating forces on the prosthesis. The latter also shows that morphology has an influence on the ligamentous structures and that their influence on prosthesis instability is intertwined. Further research on the exact role of the ligamentous structures is needed, especially to determine if capsular release is beneficial or not.

References

[1] S. Dahaghin, S.M.A. Bierma-Zeinstra, A.Z. Ginai, H.A.P. Pols, J.M.W. Hazes, and B.W. Koes. Prevalence and pattern of radiographic hand osteoarthritis and association with pain and disability (the rotterdam study). *Ann Rheum Dis*, 64(5):682–687, 2005.

[2] A.L. Armstrong, J.B. Hunter, and T.R. Davis. The prevalence of degenerative arthritis of the base of the thumb in post-menopausal women. *J Hand Surg Br*, 19(3):340–341, 1994.

[3] G.M. Vermeulen, H. Slijper, R. Feitz, S.E.R. Hovius, T.M. Moojen, and R.W. Selles. Surgical management of primary thumb carpometacarpal osteoarthritis: a systematic review. *J Hand Surg Am*, 36(1):157–169, 2011.

[4] M. Ulrich-Vinther, H. Puggaard, and B. Lange. Prospective 1-year follow-up study comparing joint prosthesis with tendon interposition arthroplasty in treatment of trapeziometacarpal osteoarthritis. *J Hand Surg Am*, 33(8):1369–1377, 2008.

[5] M.J. Robles-Molina, F. López-Caba, R.C. Gómez-Sánchez, E. Cárdenas-Grande, M. Pajares-López, and P. Hernández-Cortés. Trapeziectomy with ligament reconstruction and tendon interposition versus a trapeziometacarpal prosthesis for the treatment of thumb basal joint osteoarthritis. *Orthopedics*, 40(4):e681–e686, 2017.

[6] A.D. Ganhewa, R. Wu, M.P. Chae, V. Tobin, G.S. Miller, J.A. Smith, W.M. Rozen, and D.J. Hunter-Smith. Failure rates of base of thumb arthritis surgery: A systematic review. *J Hand Surg Am*, 44(9):728–741, 2019.

[7] S.W. Wachtl, P.R. Guggenheim, and G.R. Sennwald. Cemented and non-cemented replacements of the trapeziometacarpal joint. *J Bone Joint Surg Br*, 80-B(1):121–125, 1998.

[8] A. Brauns, P. Caekebeke, and J. Duerinckx. The effect of cup orientation on stability of trapeziometacarpal total joint arthroplasty: a biomechanical cadaver study. *J Hand Surg Eur*, 44(7):708–713, 2019.

[9] The Skeletal System. Trapezium bone. https://www.theskeletalsystem.net/arm-bones/trapezium-bone.html, 2018. Accessed: 15-06-2022.

[10] The Skeletal System. Trapezium bone surfaces and articulations. https://www.theskeletalsystem.net/arm-bones/trapezium-bone.html, 2018. Accessed: 15-06-2022.

[11] G.D. Lister, H.E. Kleinert, J.E. Kutz, and E. Atasoy. Arthritis of the trapezial articulations treated by prosthetic replacement. *Hand*, 9(2):117–129, 1977.

[12] T. Imaeda, W.P. Cooney, G.L. Niebur, R.L. Linscheid, and K. An. Kinematics of the trapeziometacarpal joint: a biomechanical analysis comparing tendon interposition arthroplasty and total-joint arthroplasty. *J Hand Surg Am*, 21(4):544–553, 1996.

[13] V. Spartacus, A. Mayoly, A. Gay, T. Le Corroller, M. Némoz-Gaillard, S. Roffino, and P. Chabrand. Biomechanical causes of trapeziometacarpal arthroplasty failure. *Comput Methods Biomech Biomed Engin*, 20(11):1233–1235, 2017.

[14] E. Gerace, D. Royaux, E. Gaisne, L. Ardouin, and P. Bellemère. Pyrocardan® implant arthroplasty for trapeziometacarpal osteoarthritis with a minimum follow-up of 5 years. *Hand Surg Rehabil*, 39(6):528–538, 2020.

[15] P. Ledoux. Revision procedures after trapeziometacarpal surgery. *Hand Surg Rehabil*, 40:143–150, 2021.

[16] M. Bricout and J. Rezzouk. Complications and failures of the trapeziometacarpal maia® prosthesis: A series of 156 cases. *Hand Surg Rehabil*, 35(3):190–198, 2016.

[17] M. Pérez-Úbeda, A. Garcia-López, F. Marco Martinez, E. Junyent Vilanova, M. Molina Martos, and L. López-Duran Stern. Results of the cemented sr trapeziometacarpal prosthesis in the treatment of thumb carpometacarpal osteoarthritis. *J Hand Surg Am*, 28(6):917–925, 2003.

[18] A. Pendse, A. Nisar, S.Z. Shah, A. Bhosale, J.V. Freeman, and I. Chakrabarti. Surface replacement trapeziometacarpal joint arthroplasty – early results. *J Hand Surg Eur*, 34(6):748–757, 2009.

[19] J. Duerinckx and P. Caekebeke. Trapezium anatomy as a radiographic reference for optimal cup orientation in total trapeziometacarpal joint arthroplasty. *J Hand Surg Eur*, 41(9):939–943, 2016.

[20] P. Caekebeke and J. Duerinckx. Can surgical guidelines minimize complications after maïa® trapeziometacarpal joint arthroplasty with unconstrained cups? *J Hand Surg Eur*, 43(4):420–425, 2017.

[21] J.S. Martinez de Aragon, S.L. Moran, M. Rizzo, K.B. Reggin, and R.D. Beckenbaugh. Early outcomes of pyrolytic carbon hemiarthroplasty for the treatment of trapezial-metacarpal arthritis. *J Hand Surg Am*, 34(2):205–212, 2009.

[22] A. Klahn, M. Nygaard, R. Gvozdenovic, and M.E.H. Boeckstyns. Elektra prosthesis for trapeziometacarpal osteoarthritis: a follow-up of 39 consecutive cases. *J Hand Surg Eur*, 37(7):605–609, 2012.

[23] T.B. Hansen and D. Vainorius. High loosening rate of the moje acamo prosthesis for treating osteoarthritis of the trapeziometacarpal joint. *J Hand Surg Eur*, 33(5):571–574, 2008.

[24] S. Lemoine, G. Wavreille, J.Y. Alnot, C. Fontaine, and C. Chantelot. Second generation guepar total arthroplasty of the thumb basal joint: 50 months follow-up in 84 cases. *Orthop Traumatol-Sur*, 95(1):63–69, 2009.

[25] O. Eiken. Prosthetic replacement of the trapezium: Technical aspects. *Scand J Plast Recon*, 5(2):131–135, 1971.

[26] R.M. Braun. Stabilization of silastic implant arthroplasty at the trapezometacarpal joint. *Clin Orthop Relat R*, 121:263–270, 1976.

[27] R.L. Linscheid. Implant arthroplasty of the hand: retrospective and prospective considerations. *J Hand Surg Am*, 25(5):796–816, 2000.

[28] S.W. Wachtl and R.R. Sennwald. Non-cemented replacement of the trapeziometacarpal joint. *J Bone Joint Surg Br*, 78(5):787–792, 1996.

[29] A. Andrzejewski and P. Ledoux. Maïa trapeziometacarpal joint arthroplasty: Survival and clinical outcomes at 5 years' follow-up. *Hand Surg Rehabil*, 38(3):169–173, 2019.

[30] B. van Hove, J. Vantilt, A. Bruijnes, P. Caekebeke, K. Corten, I. Degreef, and J. Duerinckx. Trapeziometacarpal total joint arthroplasty: The effect of capsular release on range of motion. *Hand Surg Rehabil*, 39(5):413–416, 2020.

[31] N. Dreant and M. Poumellec. Total thumb carpometacarpal joint arthroplasty: A retrospective functional study of 28 moovis prostheses. *Hand*, 14(1):59–65, 2019.

[32] P. Gonzalez-Espino, M. Pottier, C. Detrembleur, and D. Goffin. Touch double mobility arthroplasty for trapeziometacarpal osteoarthritis: outcomes for 92 prostheses. *Hand Surg Rehabil*, 40(6):760–764, 2021.

[33] B. Lussiez, C. Falaise, and P. Ledoux. Dual mobility trapeziometacarpal prosthesis: a prospective study of 107 cases with a follow-up of more than 3 years. *J Hand Surg Eur*, 46(9):961–967, 2021.

[34] A. Martins, S. Charbonnel, F. Lecomte, and L. Athlani. The moovis implant for trapeziometacarpal osteoarthritis: results after 2 to 6 years. *J Hand Surg Eur*, 45(5):477–482, 2020.

[35] G.B. Florez and R. Rubio. Carpometacarpal hemiarthroplasty. *Oper Tech Orthop*, 28(1):43–48, 2018.

A Search Strategy

PubMed

(trapeziometacarpal[Text Word] OR tmc[Text Word] OR carpometacarpal[Text Word] OR cmc[Text Word] OR "thumb bas*"[Text Word] OR "thumb metacarpal"[Text Word] OR carpometacarpal joints[MeSH Terms] OR trapezium bone[MeSH Terms]) AND (implant*[Text Word] OR prosthes*[Text Word] OR "joint replacement"[Text Word] OR arthroplast*[Text Word] OR arthroplasty, replacement, finger[MeSH Terms] OR hemiarthroplasty[MeSH Terms] OR joint prosthesis[MeSH Terms]) AND (instability[Text Word] OR unstable[Text Word] OR sublux*[Text Word] OR dislocat*[Text Word] OR displace*[Text Word] OR loosen*[Text Word] OR treatment failure[MeSH Terms] OR prosthesis failure[MeSH Terms]) AND english[Language] AND "journal article"[Publication Type]

Scopus

(TITLE-ABS-KEY (trapeziometacarpal OR tmc OR carpometacarpal OR cmc OR "thumb bas*" OR "thumb metacarpal") AND TITLE-ABS-KEY (implant OR prosthes?s OR "joint replacement" OR arthroplast*) AND TITLE-ABS-KEY (instability OR unstable OR sublux* OR dislocat* OR displace* OR loosen*) AND LANGUAGE (english)) AND (LIMIT-TO (DOCTYPE , "ar") OR LIMIT-TO (DOCTYPE , "re"))

First author, year	Country	Study design	Level of evidence	Population	Mean follow-up (months)	Prosthesis
Andrzejewski 2019	Belgium	Retrospective case series	4	113	63	Maïa
Braun 1976	USA	Case series	4	15	6-48 (no mean)	Swanson silastic
Brauns 2019	Belgium	Cadaveric study	5	N/A	N/A	N/A
Bricout 2016	France	Retrospective case series	4	156	37,8	Maïa
Caekebeke 2018	Belgium	Retrospective cohort study	4	50	65	Maïa
de Aragon 2009	USA	Retrospective case series	4	54	22	CMI
Duerinckx 2016	Belgium	Case series	3	N/A	N/A	N/A
Eiken 1971	Sweden	Expert opinion	5	N/A	N/A	N/A
Gerace 2020	France	Prospective case series	4	103	67 (median)	Pyrocardan
Hansen 2008	Denmark	Case series	4	9	12	Moje Acamo CMC
Imaeda 1996	USA	Cadaveric study	5	N/A	N/A	N/A
Klahn 2012	Denmark	Prospective case series	4	39	48	Elektra
Ledoux 2021	France	Mini review	4	N/A	N/A	N/A
Lemoine 2009	France	Retrospective case series	4	84	50	Guepar
Linscheid 2000	USA	Review	4	N/A	N/A	N/A
Lister 1977	USA	Retrospective case series	4	36	27,4	Swanson silastic
Pendse 2009	UK	Retrospective case series	4	62	36 (median)	Avanta SR TMC
Pérez-Ubeda 2003	Spain	Retrospective case series	4	20	33	Avanta SR TMC
Spartacus 2017	France	Cadaveric study	5	N/A	N/A	N/A
van Hove 2020	Belgium	Cadaveric study	5	N/A	N/A	N/A
Wachtl 1996	Switzerland	Case series	4	45	25,3	Ledoux
Wachtl 1998	Switzerland	Case series	4	43 (DLC) 45 (L)	63 (DLC) 25 (L)	DLC Ledoux